THE CONNECTION BETWEEN X-RAY AND RADIO SELECTED BL LACERTAE OBJECTS

Paolo Padovani[1] and Paolo Giommi[2]

[1] Dipartimento di Fisica, II Università di Roma "Tor Vergata", Via della Ricerca Scientifica 1, I-00133 Roma, Italy
Internet: padovani@romaz1.mi.it

[2] ESIS, Information Systems Division of ESA, ESRIN, Via G. Galilei, I-00044 Frascati, Italy
Internet: giommi@mailserv.esa.it

Accepted 1991 July 15; accepted

ABSTRACT

We explain the properties of X-ray selected BL Lacertae objects, under the assumption that they constitute the small minority of the BL Lac population with energy output located in the VUV/X-ray band as suggested by their multifrequency spectra in particular, two characteristic X-ray luminosity functions, $\log N$-$\log S$ and radio flux distribution distinting from radio selected BL Lacs using a method that does not require any free parameters. Our phenomenon is in tension with the most common explanation for the existence of two classes of BL Lacs, namely that X-ray selected objects are viewed significantly off the persistent axis while radio-selected ones have their jets more aligned with the line of sight. In this case, in fact, X-ray selected sources should be intrinsically more numerous than objects selected in the radio band as a fixed ratio of some isotropic luminosity such as that of the radio emission. We also account for most of the properties of BL Lacs detected in current X-ray surveys, this latter scenario would predict their radio emission to be dominated by the extended (unpaired) component, in contrast with observations. We also address the duration of the negative evolution apparently exhibited by X-ray selected BL Lacs, showing that neither recognition biophcans nor a peak in the X-ray spectrum are likely to be responsible for it. Our phopthesis explains in a simple way the bimodal distribution of BL Lacs in the $\alpha_{ox} - \alpha_{ox}$ diagram. It also makes specific predictions for the X-ray, radio and optical properties of BL Lacs with flux below the peaked by infrared deep X-ray surveys.

Subject Headings: Galaxies: BL Lacertae Objects: general — radio continuum: Galaxies — X-rays: Galaxies

1. INTRODUCTION

The extreme properties of BL Lacertae Objects[5] are often separated from most other types of active galactic nuclei (AGN). Namely, BL Lacs are core-dominated radio sources (e.g. Antonucci & Urrestad 1982; Fermani & Stocke 1995) displaying superluminal motion on very long baseline interferometry (VLBI) maps (see e.g. the compilation by Vermeulen & Cohen 1994). Following Giroldi et al. (1999) we define a BL Lac as a flat spectrum radio source with redshift-frame luminosity at 5 GHz $< 5 \times 10^{24}$ W Hz^{-1}. This is the same limit applied by Stocke et al. (1991) to the observed equivalent width of the strongest line < 5 Å. The selection of BL Lacs from the Einstein Operations Extended Medium Sensitivity Survey

[5] Following Giroldi et al. (1999) we define a BL Lac as a flat spectrum radio source with

Cohen 1964), and characterized by high variability and relatively high optical polarization (e.g. Angel & Stockman 1980; Lamastra, Smith & Elston 1994). The property which distinguishes them most from other AGN is, however, their almost complete lack of emission lines. This feature has led to the simplest idea, that, contrary to most other astronomical sources, BL Lacs have been almost exclusively directed at radio or X-ray frequencies (X-ray-selected BL Lacs). The sometimes different properties of the two subclasses have led to the view that BL Lacs come in two flavors, according to their selection band. In itself, among currently known objects, XBLs are more core dominated, highly polarized, variable, and luminous (at radio and optical frequencies) than XBLs (e.g. Fossati et al. 1998; Sambruna et al. 1996; Morris et al. 1991; Padovani 1992a). The two classes also occupy different regions on the $\alpha_{ro} - \alpha_{ox}$ plane, which is indicative of different energy distributions (Stocke et al. 1985; Laskar & O'Dell 1985). Moreover, whereas XBLs show a weak positive correlation, consistent at the 3σ level with no evolution (Giommi et al. 1991), XBLs display a negative correlation, that is they seem to have been less abundant and/or less luminous at higher redshifts, although very in this case zero evolution is excluded only at the ~ 3σ level (Wolter et al. 1994; but see also § 4.5). We note that summary NCN negative evolution is a property unique to XBLs.

The properties of BL Lacs have been explained in terms of relativistic beaming, that is these objects are thought to be low luminosity (i.e. Fanaroff-Riley type I; Fanaroff & Riley 1974) radio galaxies dominated by emission from a relativistic jet closely aligned with the line of sight (e.g. Urry & Padovani 1995). Within this scenario, the less extreme properties of XBLs have been attributed to a larger viewing angle (e.g. Stocke et al. 1985): for example, XBLs would be less luminous than XBLs in the radio and optical band because they are viewed off the peaming axis. The similar X-ray luminosities of XBLs and RBLs have been lifted into this picture by assuming that the X-ray beam is produced than the radio\optical beam (Maraschi et al. 1986), either because the Lorentz factor of the X-ray emission is smaller than that the one of the radio emission ("Accretion Jet" model: Ghisellini & Maraschi 1989; see also Padovani & Urry 1990) or because the jet is more collimated at lower frequencies ("Wind Jet" model: Celotti et al. 1993). At a given X-ray flux, or luminosity, XBLs should then outnumber RBLs (simply because the probed beams make it more likely that one line of sight intercepts their jets), as effectively derived from their X-ray number counts (Urry, Padovani & Stickel 1991) and luminosity function (Celotti et al. 1993). In this framework, RBLs are viewed within ~ 10° − 15° from the line of sight, while the relativistic jets in XBLs are oriented at larger angles ~ 15° − 30° (e.g. Urry & Padovani 1995). XBLs are often about an order of magnitude more numerous than RBLs.

In the following, we will refer to this picture as the „Different Viewing Angle" phenomena.

The division of BL fascicles into KBLs and XBLs is clearly not established, since entry (Eire et al. [1991]) an X-ray survey covering most of the sky, has detected many BL Lacs that were also found in radio surveys. These sources could now be employed as KBLs or XBLs. Approaching the problem from a more physical point of view, Giommi & Ansari & Micol (1995) have studied the multiwavelength spectrum of a large sample of BL Lacs. They state that there was no only one proportion of objects, characterized by a white range of energy cutoffs: at intermediate-optical energies for most KBLs, at VU/X-ray or higher energies for most XBLs. Furthermore, objects with high-energy cutoff constitute about 70% of KBLs: since radio selection should be unbiased with respect to the cutoff energy, Giommi et al. (2001) conclude that black energies in the ultraviolet to X-ray band are rare; it follows that BL Lacs of the XBL type (i.e. those where the cutoff is at VU/X-ray frequencies) would constitute a minority of the BL Lac population. This is consistent with the fanciful reported to as the „Different Energy Cutoff" phenomena. Note that in this case the elimination is reversed with respect to the „Different Viewing Angle" phenomena which, as mentioned before, requires XBLs to constitute the majority of BL Lacs. We explain this apparent contradiction as a simple selection effect (see Giommi & Padovani 1995 and § 3.1).

In a previous paper (Giommi & Padovani 1994, personal Paper I), we have shown that within the „Different Energy Cutoff" scenario, the X-ray counts of XBLs can be reproduced starting from the radio counts of KBLs. The purpose of this paper is to extend the work of Paper I by defining the statistical properties of XBLs starting from a population of BL Lacs of the KBL type. Namely, in § 5 we describe in detail our phenomena and assumptions; in § 3 we compare the X-ray luminosity function (LE), radio properties and redshift distribution of XBLs, computed according to our picture, with the observational data. In § 4 we tackle the problem of the negative correlation of XBLs, while in § 6 we examine critically now other operational properties of XBLs in in the „Different Energy Cutoff" and „Different Viewing Angle" scenario. The distribution of BL Lacs on the $\alpha_{ox} - \alpha_{io}$ plane is explained within our phenomena in § 6. Some predictions for future X-ray surveys are given in § 7, while in § 8 we discuss and summarize our conclusions.

As in Paper I, we will use the terms „KBLs" and „XBLs" when we refer to the selection band, and „KBL-like" and „XBL-like" when we refer to their energy distribution. The adopted cosmology uses parameters $H_0 = 50$ km s^{-1} Mpc^{-1} and $q_0 = 0$ (Giommi et al. [2001]) is taken based on examination of the energy distributions given by Giommi et al.

to be $\lambda/\lambda \simeq 10^{-11}$, where X-ray fluxes cover the 0.3 – 3.2 keV range and are in units of erg cm^{-2} s^{-1}, and radio fluxes refer to 2 GHz and are expressed in Janskys (this corresponds, with $\sigma_x = 1$, to $\sigma_{xx} \simeq 0.17$ between 1 keV and 2 GHz). Due to obvious selection effects most (but not all) XBRs are XBL-like and most (but not all) BRLs are BRL-like. Throughout this paper the adopted $H_0 = 20$ km s^{-1} Mpc^{-1} and $\Omega_\Lambda = 0$ flat geometry and spectral indices are written $\lambda \propto \nu_{-\sigma}$.

3. THE "DIFFERENT ENERGY CUTOFF" HYPOTHESIS

Our hypothesis has been defined in Paper I: we summarize here the main points. We assume that BL Lacs are a single family of objects characterized by a smooth energy distribution (broadly due to the synchrotron mechanism) from radio to infrared (IR) frequencies followed by a sharp cutoff that is often located in the IR\/Optical band but more rarely ($\simeq 10\%$ of the cases) in the Ultraviolet\/X-ray band; above this cutoff the emission is much lower and is broadly due to Synchrotron Self Compton (SSC) emission. Under this hypothesis, in Paper I we have derived the X-ray counts of XBRs from the radio counts of BRLs controlled with the bivariate distribution of the ratios of X-ray to radio flux, $P_\lambda(\lambda_x \backslash \lambda)$ (eq. 1 of Paper I). More generally, some properties of XBRs can be derived from the conformation of the radio counts (luminosity function) of BRLs with the bivariate distribution of the ratios of X-ray to radio flux (luminosity). We discuss these two investigations in turn.

3.1 The Radio Luminosity Function and Counts of XBRs

Our approach requires the knowledge of the radio counts of XBRs down to at least ~ 1 mJy, the minimum radio flux of the XBRs discovered so far, while the only complete excellent sample of XBRs has a flux limit of 1 Jy at 5 GHz. Moreover, the counts cannot be derived from the observed radio LF of XBRs since this is only extended down to $P_{5GHz} \sim 10^{32}$ W Hz^{-1} (Giliokis et al. 1999), while XBRs can have radio powers as robust as those of measured (e.g. Wolter et al. 1994). Deep radio counts for XBRs were then derived from the radio LF, predicted by the pseudo model, which fits the observed LF of the 1 Jy sample and extends down to $P_{5GHz} \sim 10^{31}$ W Hz^{-1} (Urry et al. 1999). We treat slant with the assumption of no evolution for BL Lacs as a class, which is consistent at the $\sim 5\sigma$ level with the observational data for both XBRs and BRLs (the direction of the negative evolution approach exhibited by XBRs will be addressed in § 4). Since the peak-IR LF evolution approach optimized by Urry et al. (1999) was based on the peak-IR (boosting) evolution found by

Shikel et al. [1991] we rederived the radio LE predicted by the dynamic model by lifting the operator LE correspondence to the nonrotational case. To this aim, we first derived the local radio luminosity function for the I ty sample assuming no evolution. Shikel et al. [1991] give tabulated s for 52 I ty BL Lacs, one more (that is of 0.242+244 saw taken from Shikel, Mckenzie-Smith & Kühr (1994)) for BL Lacs near power limits from spectroption lines; this non more have only a power limit of $z < 0.5$ obtained from the shell appearance of their optical images (Shikel et al. 1991). For the purpose of the LE derivation, we have set the low power limits $z > 0.0$ of the sample to $\langle z \rangle = 36.0$ [the mean value for the whole sample derived taking into account the presence of power limits using VSUPA K.r. (KaWalk), Isope & Ferguson (1991)] which underestimate the methods presented in Eigelson & Nelson (1992)] and considered the other low power limits as actual estimates. We note that these assumptions affect the shape of the LE at high powers ($\lesssim 2 \times 10^{25}$ W Hz^{-1}) and therefore have only a small influence on the total number density. Finally, the radio LE predicted by the dynamic model was derived from a fit to the observed one as described in Urry et al. (1991). The fit and the data are shown in Figure 1. Differential radio counts were obtained from the radio LE assuming $\rho_z = -0.75$, the mean value for the I ty sample, and $z^{max} = 5$.

3.3. The k/k Distribution for BL Lacs

The derivation of the distribution of ratios of X-ray to radio flux overlaps requires X-ray and radio fluxes for BL objects in the two complete BL Lac samples we employ, i.e. the I ty (Shikel et al. 1991) and the Einstein Observatory Extended Medium Sensitivity Survey [EMSS] (Stocke et al. 1991) samples. X-ray and radio data for the EMSS BL Lacs are given by Stocke et al. (1991). In Paper I, X-ray data for I ty BRLs were taken from Padovani (1992a) (and references therein), i.e. the X-ray fluxes in the 0.3 − 3.5 keV range (which is the X-ray band of the EMSS BL Lacs) were derived from the fluxes at I keV using the appropriate spectral index Γ, or $\alpha_x = 1$ (Worrall & Wilkes 1990). The high energy (HE) and HEAO-1 SA data. This can lead to biases when constraint to the 0.3 − 2.4 keV energy range, since the former and the latter are respectively soft (0.02 − 0.5 keV) and hard (3 − 10 keV) when the Einstein band. To obtain more homogeneous X-ray data we decided to facilitate the comparison with the X-ray data of EMSS BL Lacs we decided to

contrasts on Einstein VLC observations. The Einstein datapaths were then scanned with the European Space Information System (ESIS; Giommi et al. 1999) and X-ray data were found for twenty-two I ly BL Lacs. Uncertainties derived from counts simply multiplying by 3×10^{-11}, which is appropriate for column densities and spectral indices typical of BL Lacs. When multiple observations were available, we took a mean value if the variations were small. Then about a factor of 5. Afterwards, we used the smallest count rate in Keplerian with the results of Giommi et al. (1999) that BL Lacs, on average, spend less than 20% of the time in flares that involve X-ray flux variations of factors of 3 or more. (Note that, as also discussed in paper I, the specific procedure for dealing with X-ray variability does not significantly influence our results.) Where possible, we also checked that these typical values were roughly consistent with those found by Giommi et al. (1999) with EXOSAT. X-ray data for 8 more BL Lacs were optained from ROSAT counts given by Sambruna et al. (1996) for a large band of the I ly sample. For one object (0120–2610) on Einstein or ROSAT data were found but an upper limit optained with the HEAO-1 experiment (Della Ceca et al. 1999) shows it to belong to the XBL-like class.

As described in Paper I, a key value for our derivation of the $\lambda_x \backslash \lambda$ distribution for the whole BL Lac population is the ratio between XBL-like and XBL-like objects in radio selected samples. This ratio is 16 (35\5) for the I ly BL Lacs (the two XBL-like objects being MKN 106 and PKS 2005–489). In trying to reduce the statistical noise we employed two other radio samples of BL Lacs, namely the 2Jy ($\lambda \leq 0.2$ ly at 2 GHz: Stickel & Kühr 1994) and the 35 samples ($\lambda \leq 0.35$ ly at 2 GHz: Kühr et al. 1981; Stickel, Bryant & Kühr 1994) of 2Jy BL Lacs, respectively. X-ray data are available for 11 out of 14[4] 2Jy BL Lacs, but the terminline communication). X-ray data are available for 11 out of 14 2Jy BL Lacs, but the terminline three objects are multiply to be of the XBL-like type: in that case, in fact, they should have been detected in the Einstein HRC Slew survey (Elvis et al. 1992). We derive a ratio of XBL-like to XBL-like objects ~ 0 (5\51) for the 2Jy sample. As regards the 35 BL Lacs, X-ray data are available for 11 out of 13 objects and even in this case the terminline two objects should have disappeared been detected in the Einstein HRC Slew survey. Bad they been of the XBL-like type. The ratio of XBL-like to XBL-like objects for the 35 sample is ~ 51 (1\51). In the following we adopt for the ratio of XBL-like to XBL-like objects in radio samples the mean value for the three samples $\simeq 10$; the (conservative) range for this ratio

[4] Note that 1525+528 (MKN 501) and 2344+514 have been marginally classified as a QSO respectively in the 2A catalog (Stickel & Kühr 1994): both (normal) galaxy and a QSO respectively in the 2A catalog (Stickel & Kühr 1994): both objects are in fact I ly BL Lacs. The number of 2A BL Lacs increases then from twelve to fourteen.

is $0 - 10$.

The $\lambda_x \backslash \lambda$ distribution for the whole BL fac population, $\mathrm{P}(\lambda_x \backslash \lambda)$, was usually derived by adding up the fractional $\lambda_x \backslash \lambda$ distribution of 1 yr KBLs that to EMSS XBLs weighted (reduced) by a factor of 10. In doing so, as noted in Paper I, we are trying to estimate the XBL-like tail of the $\lambda_x \backslash \lambda$ distribution, underestimated by the 1 yr KBLs. The final distribution was then re-normalized so that $\int \mathrm{P}(\lambda_x \backslash \lambda) d(\lambda_x \backslash \lambda) = 1$ and is shown in Figure 5. We note that $\mathrm{P}(\lambda_x \backslash \lambda)$ is somewhat different from the one optained in Paper I but our ideal derivation is more reliable because it includes all 1 yr KBLs and also because the $\mathrm{E.B.-E.B.}$ Key Plots were derived directly from the counts. The lack of objects with $\lambda_x \backslash \lambda$ $0.0 \leq \mathrm{E.B.-E.B.} \leq 0.1$ is probably due to small statistics and the sensitivity status of the EMSS survey (see § 3.3). This is confirmed by the fact that 2 BL Lacs out of the 44 identified so far in the Einstein IPC Slew survey (Elvis et al. 1992; Schachter et al. 1993) fall in this range. However, our main results are not very sensitive to the exactly shape of the $\lambda_x \backslash \lambda$ distribution in this interval. Note also that we assume no evolution of $\mathrm{P}(\lambda_x \backslash \lambda)$, *i.e.* no dependency on redshift and\or luminosity.

3. RESULTS

In this section we compare some predictions of the "Different Energy Cutoff" hypothesis with observations; also commenting briefly on how the "Different Variable Index" hypothesis explains the same data. We emphasize that even if our hypothesis were 100% correct, we would not expect perfect agreement between calculated and observed properties. This is because of the inevitable uncertainties intrinsic to the two ingredients of our scheme: the radio LE of KBLs which, although based on a model with reasonable well the operated LE, significantly extends below it; and the $\lambda_x \backslash \lambda$ distribution for the whole BL fac population, whose determination ideally would require a large (and deep) radio sample (see Paper I). Finally, X-ray variability adds further "noise" both to our predictions and to the data. We point out that in our scenario we have no free parameters.

3.1. X-ray Number Counts

The X-ray number counts predicted by our hypothesis have been presented in Paper I. We show in Figure 3 our latest results optained following eq. (1) to Paper I and using the newly derived $\lambda_x \backslash \lambda$ distribution. The predicted X-ray counts are in agreement with results from various X-ray surveys (see Figure 3 we also present the "pristine" X-ray counts for the 1 yr KBLs, derived simply assuming to each object its X-ray flux, as derived

in § 5.5, and his number density is defined from its radio flux in the I γγ energy (Zirakel et al. [1991]). In our scenario, as attested in Figure 1, XBLs seem to outnumber I γγ BBLs by a factor of two classes sample different behaviour of the BL Lac radio counts. As a consequence of their higher $\lambda_{\rm x}\backslash\lambda_{\rm r}$ ratios, in fact, XBL-like objects have lower radio fluxes (∼ 10 mJy) and since faintest objects are more numerous than brighter ones (the radio counts are steeper), their surface density is higher. Zirakel differently, X-ray energy sample the BL Lac radio counts at low fluxes and mostly detect the ∼ 100% of objects with high $\lambda_{\rm x}\backslash\lambda_{\rm r}$ ratios. ATF distinguishes more works down to an X-ray flux $\bar{\lambda}_{\rm x} \simeq \lambda_{\rm r,lim} \times (\lambda_{\rm x}\backslash\lambda_{\rm r})_{\rm lim(XBL-like)}$ ratios. ATF distinguishes more works down to an X-ray flux $\bar{\lambda}_{\rm x} \simeq \lambda_{\rm r,lim} \times (\lambda_{\rm x}\backslash\lambda_{\rm r})_{\rm lim(XBL-like)}$ ratios: $\lambda_{\rm r,lim}$, where $\lambda_{\rm r,lim}$ is the radio flux at which the radio counts of BBLs converge: $\simeq 10^{-11}$ Jy at least fluxes X-ray surveys should find only BBL-like objects since all XBL-like objects will have steeper radio defected. The process name of $\lambda_{\rm x}$ depends from on the definitions of the radio LE of BL Lacs at very low powers, which is clearly drive uncertain: usually the LE defined in § 5.1 one optimus an X-ray flux orders of magnitude below the deepest ROSAT surveys. As a consequence of the fact that BBL-like objects will at the end dominate, being intrinsically more numerous, their fraction should slowly increase in X-ray surveys as shown in Figure 1 (Fig. 5).

We notice that the "Different Viewing Angle" hypothesis also explains the observed X-ray number counts of BL Lacs (Padovani & Giommi [1995]).

4.4 X-ray LF

The procedure followed to predict the X-ray LF for XBLs is similar to that adopted for the derivation of the number counts. Namely, we first obtained the $\lambda_{\rm x}\backslash\lambda_{\rm r}$ distribution for BBLs and XBLs, where $\lambda_{\rm r}$ is the X-ray luminosity in the 0.5 − 2.5 keV band and $\lambda_{\rm r}$ is the radio power at 5 GHz. A spectral index $\alpha_{\rm x} = 1$ was assumed for both BBLs and XBLs, while radio spectral indices between 0.7 and 5 GHz for BBLs were taken from Giroletti et al. [1991]. A redshift XBLs, spectral indices between 0.5 and 5 GHz were derived for 12 EMSS BL Lacs from the data given in Perlman & Stocke [1993] and Stocke et al. [1991], while for the remaining objects the mean value $\alpha_{\rm r} = 0.50$ was assumed. The bropsplitt distribution for the whole BL Lac population $\Phi_{\rm r}(\lambda_{\rm x}\backslash\lambda_{\rm r})$ was then optained by adding to the normalized distribution of BBLs that of XBLs weighted by a factor of 10, as derived in § 5.5. The X-ray LE of XBLs, $\phi_{\rm x}(\lambda_{\rm x})$ is then related to the radio LE of BBLs, $\phi_{\rm r}(\lambda_{\rm r})$, (derived in § 5.1) through the following equation:

$$\phi_{\rm x}(\lambda_{\rm x}) = \int_{\lambda_{\rm r,min}(\lambda_{\rm x})}^{\lambda_{\rm r,max}(\lambda_{\rm x})} \phi_{\rm r}(\lambda_{\rm r}) \Phi_{\rm r}(\lambda_{\rm x}\backslash\lambda_{\rm r}) d\lambda_{\rm r}. \quad (1)$$

where $\lambda_{x,\min} = \lambda_x \backslash (\lambda_x \backslash \lambda_1)^{\max}$ and $\lambda_{x,\max} = \lambda_x \backslash (\lambda_x \backslash \lambda_1)^{\min}$.

We compare our predictions with the χ-ray LE for the EMSS subsample of 30 BL Lacs with $\lambda_x \leq 5 \times 10^{-12}$ erg cm^{-2} s^{-1} (Wolter et al. 1991). We followed the method of Ariri & Bellazzini (1991) to take into account the fact that the volume entropy in the EMSS is a function of luminosity lux. Redshifts, luxes, and sky coverage were taken from Wolter et al. (1991). Two objects in the sample have no redshift determination: these were initially excluded from the sample but their presence was taken into account by multiplying the normalization of the resulting LE by $30\backslash 28$. In keeping with the assumption of no evolution for the BL Lac class, no evolutionary corrections were made in the derivation of the LE.

The χ-ray LE predicted by our phyporheis is shown in Figure 4. Our predictions are reasonably consistent with observations: a formal χ^2_5 analysis gives $\chi^2_5 \simeq 5.5$, which (Flocke, private communication: 10 objects happen to end up in the first bin, i.e. the one which dissences most with the predicted LE), and remarkably by the factor $30\backslash 23$. The χ^2_5 would of course decrease very further if one took into account the possible range tempered χ^2_5 would of course decrease very further if one took into account the possible range of normalization in our predicted LE of a factor of $\sim 2^{0.5}$ due to the corresponding range in the weighting factor ($i.e.$ the ratio of BL-like to XBL-like objects in radio samples) derived in § 5.5 ($\theta = 1$). In Figure 4 we also show the LE for BL-like objects to be bound in χ-ray energy. As in the case of the number counts, their function is predicted to increase with decreasing luminosity until they outnumber XBL-like objects. This happens at $\lambda_x \simeq 10^{40} - 10^{42}$ erg s^{-1}, but this value is quite uncertain since it depends on the low luminosity bent of the radio LE derived in § 5.1. Note that the χ-ray LE of BL-like objects has to fit, by construction, the privative χ-ray LE of the 1 γ BL Lacs of the RBL type: the former is in fact derived from eq. (1) using $\eta(\lambda_x \backslash \lambda_1)(\mathrm{BL\text{-}like})$, which coincides with the $\lambda_x \backslash \lambda_1$ distribution of the 1 γ sample (excluding the two XBL-like objects). It $\phi_{\gamma}(\lambda_x)$ fits the observed radio LE of the 1 γ BL Lacs, $\phi_X(\lambda_x)$ optained from eq. (1) will then fit their privative χ-ray LE.

The predictions of the "DiCicart Newring Angle" phyporheis seem also to fit the χ-ray LE of the EMSS BL Lacs derived for the minimal evolution allowed by the data, i.e. perfectly for the zero evolution case (Colotti et al. 1991; Wolter et al. 1991). The χ-ray LE for BL-like objects is in their model, simply equal to that of XBL-like objects scaled down by the number density ratio between the two populations: the slope of the two χ-ray LEs is then predicted to be the same, with XBL-like objects outnumbering BL-like ones in all χ-ray luminosities, at variance with our results.

Our approach allows us also to predict the radio properties of XBLs. For example, the radio flux distribution (per line strength) of an X-ray selected sample is a tight X-ray flux distribution (see Figure 6). Since it displayed in Figure 2, which shows that the EMSS BL Lacs cluster around the predicted mean relationship between radio and X-ray flux. In particular, the strong correlation observed between two fluxes for the EMSS BL Lacs (significant at the 99.99% level) is consistent with the predictions. It can be noted in the figure, however, that the observed distribution for $\lambda_x \sim 10^{-11}$ erg cm^{-2} s^{-1} Å^{-1} all the EMSS BL Lacs are below the predicted mean relationship, while for $\lambda_x \gtrsim 6 \times 10^{-11}$ erg cm^{-2} s^{-1} the EMSS BL Lacs are above the predictions, i.e. they all have radio fluxes smaller than the predicted values for this X-ray flux, while for $\lambda_x \sim 10^{-11}$ erg cm^{-2} s^{-1} Å^{-1} the EMSS BL Lacs are above the predictions, i.e. they have radio fluxes larger than the predicted values. We interpret these differences as follows: objects with relatively high X-ray and radio fluxes are missing because they were brought well known BL Lacs closer as they are in the TeV operations and therefore excluded by definition from the EMSS, that only includes serendipitous sources. A research objects with relatively small X-ray and radio fluxes, we think that more sensitive effort applies: Perrone & Marchã (1991) have suggested that the EMSS might miscalssify some optically faint BL Lacs whose light is swamped by the host galaxy, which is typically a bright elliptical. ¶ We would affect more and more objects for progressively smaller X-ray fluxes (see Figs. 6). 6 and in particular those with faintest optical fluxes. Given the correlation between radio and optical luminosities of BL Lacs (Nonino et al. 1991; Padovani & Giommi, 1995) at low X-ray fluxes the EMSS could be biased against the BL Lacs with the smallest radio fluxes. ¶ Perrone & Marchã effect" (with it influence also on $\langle \nu_m \backslash \nu \rangle$ be like described in detail in § 4.

Figure 2 shows also the location of the 1 ¶ BL Lacs on the radio flux – X-ray flux plane. Since a radio flux limit of 1 ¶ is relatively high, the dynamic range is small and most objects appear to be "bandpass" near the survey limit. Note also that RBLs and XBLs cannot be easily distinguished by X-ray fluxes only because the 1 ¶ flux limit and the $\langle \lambda \backslash \lambda_{min} \rangle$ are

line diagram to interest around $\lambda \sim 10^{21}$ erg cm^{-2} s^{-1}.

As noted in Figure 1, we can also calculate the radio flux distribution (per unit area) in an X-ray-limited sample ($\lambda \leq \lambda_{\rm lim}$), given by the integral with respect to the X-ray flux of eq. (5):

$$\Omega(\lambda) = \int_{\lambda_{\rm min}(\lambda)}^{\lambda_{\rm max}} \nu_{\rm c}(\lambda)\eta(\lambda)\phi(\lambda|\lambda_{\rm x})d\lambda_{\rm x}, \tag{3}$$

where $\lambda_{\rm x,lim}$ and $\lambda_{\rm x,max}$, respectively defined, give the X-ray flux ranges which contribute to the radio flux distribution. Multiplying eq. (3) by the area surveyed or convolving the integrand with the appropriate sky coverage gives the radio flux distribution of pc expected in an X-ray survey.

We have done this calculation using the sky coverage of the ESSS BL Lac sample to Wolter et al. (1991). Figure 6 shows the comparison between our predicted radio flux distribution and the observed one for that sample: we predict a mean value of 2.3 mJy, quite close to the observed one of 1.9 mJy. The two distributions, however, are only marginally consistent (a Kolmogorov-Smirnov [KS] test gives a 1%4% probability that they are different). This is partly because we model expect more objects with $\lambda \lesssim 60$ mJy (which are not observed) but mostly because we would expect more objects with $\lambda \gtrsim 2$ mJy than are observed. In particular, no ESSS BL Lac has a radio flux $\gtrsim 1$ mJy. As discussed above, we attribute the first difference to the extrapolations inherent in the survey and the second to the incompleteness effect discussed by Browne & Marchã (1991; see § 4 for more details).

We have also predicted the radio flux distribution to be expected in the Einstein IPC Slew survey (Elvis et al. 1991 using the sky coverage derived by Schachter, Elvis & Szentgyorgyi (1991) for the high-latitude sky ($|b| \leq 30°$, excluding also the large Magellanic Cloud [LMC], Small Magellanic Cloud [SMC], and M31 (LM31). X-ray fluxes were derived assuming BL Lacs detected so far (Elvis et al. 1991; Schachter et al. 1991a) were optimal as before multiplying by 3×10^{-11} the IPC count rates. Radio fluxes for the 77 high-latitude BL Lacs detected so far (Elvis et al. 1991; Schachter et al. 1991a) were obtained from Fricke et al. (1991), Schachter et al. (1991), Giommi et al. (1991), and cross-correlating the Slew survey with various radio catalogs using ESIS. The predicted and observed distributions are compared in Figure 7. Despite the fact that the Slew survey is little not completely identified, our predictions agree well with the sample and the range of all radio flux distribution: a KS test gives only a 45% probability that the two distributions are different. This is at ably with our results for the ESSS sample, but we think this can be understood if we consider that: 1. the Slew Survey does not sample the high-luminosity BL Lacs, which are the most powerful radio sources that were chosen as targets of the Einstein IPC survey (Elvis et al. 1991; Schachter et al. 1991a; Giommi et al. 1991). Also, the Slew survey is not complete, and the sample may be biased in favor of the brightest objects, which are the most powerful radio sources.

the Einstein operations (i.e., it is not a scrambling unitary); 3. given its latent high max limit, this unitary is essentially not affected by recognition tropkins a la Browne 2. March, which would produce a depth of 8 sources at low radio flux. ~ 70 predict 10 high-latitude BL Lacs in the 2few survey, as compared to the 75 identified so far, which is consistent with the fact that the survey is still not completely identified, especially at multiple declinations, but that $\sim 98\%$ of the BL Lacs detected have $z > 0$.

The radio LE of XBL-like objects in our scenario is easily derived: since they represent $\sim 90\%$ of KBLs but we have assumed that fraction to be independent of redshift and/or luminosity, their radio LE should be equal to that of KBLs scaled down by a factor of ~ 10. Their identify should be compared with the radio LE of XBL-like objects found in radio surveys, is present a negligible number (two objects in the 1 yr sample). The latter, however, should be approximately equal to the pristine radio LE of XBLs, derived for the EMSS BL Lacs by Colafrancesco et al. (1991) and Wolter et al. (1991) for the minimal emission followed by the data. That result results again with our predictions, in that in the (same) region covered by the two radio LEs are similar and the XBL one is indeed scaled down by about an order of magnitude from the KBL one. The interpretation of these results is twofold: the "Different Viewing Angle" hypothesis is of course different: despite the fact that XBLs are intrinsically more numerous in their model, the radio amplification is lower because these objects are seen MH their radio axis but so their radio LE is shifted to lower radio power, similarly a number darkly effect (Colafrancesco et al. 1991).

5.4 Redshift Distribution

The redshift distribution expected under our hypothesis for the Wolter et al. (1991) sample ($\lambda \leq \xi \times 10^{-21}$ erg cm^{-2} s^{-1} Hz^{-1}) were derived from the X-ray LE obtained in §.5.2 assuming $\alpha = 1$, $z_{max} = 5$ and no evolution. This was then convolved with the sky coverage of the sample and compared with the redshift distribution of the 55 EMSS BL Lacs with firm redshifts. Two predictions are inconsistent with observations, as shown in Figure 8. (Note that the shape of the predicted redshift distribution is peculiar unchanged for the ratio of KBL-like to XBL-like objects in radio samples ranging from 0 to 10.) That is mentioned in the introduction, the evolution which fits best the raw but unexpected: as mentioned in the introduction, the evolution which fits best the EMSS sample is a negative one, i.e. XBLs seem to be more abundant and/or luminous at lower redshift. This explains why our predictions, which assume zero evolution, fail to explain the observed redshift distribution of the Wolter et al. (1991) sample. In the next section we investigate possible causes of the apparent negative evolution of XBLs.

4. THE NEGATIVE EVOLUTION OF THE EMSS BL LACS

4.1 The Evolution of BL Lacs

We have mentioned in the introduction that while 1 Ty BRLs show a weak positive evolution, consistent at the 5σ level with no evolution ($\langle V/V_m \rangle = 0.00 \pm 0.02$; Schmidt et al. 1991), XBLs display a negative evolution ($\langle V/V_a \rangle = 0.36 \pm 0.02$; Wolter et al. 1991). For example, for a luminosity evolution of the form $L_x(z) = L_x(0)\exp[x\tau(z)]$, where $\tau(z)$ is the look-back time, Wolter et al. find for their sample of XBLs a best fit value of $x = -0.7$ with a 5σ range of $0.21-0.3$, consistent at $\sim 5\sigma$ level with zero evolution (as is the case for BRLs). For comparison, Schmidt et al. (1991) found for their sample of 1 Ty BRLs $x = 3.3$ ($c = 1/\tau$ in their notation) with a 1σ range of 1.7–4.5. The positive evolution of 1 Ty BRLs should be taken with care because of the relatively small statistics and significance. Furthermore, for the together BL Lacs of the 5σ survey we derive $\langle V/V_m \rangle = 0.44 \pm 0.08$, i.e. a value < 0.5 but consistent with zero evolution at the $\sim 1\sigma$ level. As regards XBLs, our method of deriving the properties of XBLs starting from those of BRLs does not introduce any dependence on redshift or luminosity. The evolutionary properties of XBLs are therefore expected to be the same as those of BRLs. In trying to reconcile their seemingly different evolutions within our phoptheses we need then to consider effects that are local to the X-ray band, such as incompleteness due to recognition problems (Browne and Marchã 1991) and K-corrections.[6] To perform unbiased this issue we have carried out extensive simulations of X-ray surveys starting from the observed properties of BL Lacs selected in the radio band under the assumptions described in § 5. Note that the "Different Viewing Angle" phopthesis does not provide any explanation for the different evolution of BRLs and XBLs.

[6] The evolutionary properties of a sample can be characterized by the mean value of the ratio between V, the volume enclosed by an object, and V_m, the maximum accessible volume within which the object would have been detected above the flux limit of the sample. In the absence of evolution V/V_m has the property of being uniformly distributed between 0 and 1, with a mean value of 0.5. When the survey is made up of separate fields with different flux limits, as is the case for the EMSS, it is more appropriate to use $\langle V/V_a \rangle$, where V_a is the ratio between the volume enclosed and available volume (Avni & Bahcall 1980). That is the ratio between the volume enclosed and available volume (Avni & Bahcall 1980).

[6] We assumed the sample to be also optically limited with $m_{lim} = 20$, as is the case for the 1 Ty sample, and we assigned $z = \langle z \rangle = 0.55$ to the three objects (1ES 0806+524, 1ES 1101−232, and 1ES 1426+428) without a redshift determination. Note that this has only a small influence on V/V_m.

Simulations of X-ray energy spectra were performed as follows. Using the Monte Carlo method we took a value of the redshift and radio luminosity along the radio TL of RBLs derived in § 3.1, i.e. the extrapolation to low powers of the best fit TL of the 1 Ys sample assuming no evolution. We then took a value for the X-ray flux of this simulated radio source using the distribution of $\lambda_x \backslash \lambda_r$ derived in § 3.3. The BL Lac so simulated is accepted as part of the X-ray survey if its X-ray flux is above the chosen survey limit. Even if the source is accepted it might not be recognized as a BL Lac because of the effect described by Browne & Marchã (1999). To take this effect into account, for every accepted source we assign an appropriate misidentification probability drawn a value from the observed distribution to ratios of X-ray to optical flux ($\lambda_x \backslash \lambda_o$) that is appropriate for its $\lambda_x \backslash \lambda_r$ ratio. We have estimated the $\lambda_x \backslash \lambda_o$ distributions by plotting the $\lambda_x \backslash \lambda_r$ distribution for 1 band by multiplying the normalised histograms of observed values in every mid mom of the 1 Ys sample and from the EMSS survey. Optical data for 1 Ys KBLs were taken from Padovani (1992a) (and references therein) while those for the EMSS BL Lacs are from Stocke et al. (1991). Once the redshift and the apparent vr of the BL Lac are known, the magnitude of its parent galaxy is optained by applying the Monte Carlo method to the expected magnitude distribution for giant ellipticals derived in Browne & Marchã (1993). Given the redshift and magnitudes of the BL Lac and of its parent galaxy we apply the prescriptions of Browne & Marchã to establish whether the BL Lac is recognized as such or it is misidentified because of the dominance of the parent galaxy. In simulating the Einstein EMSS we have taken into account the sky coverage as given in Wolter et al. (1991) by minimum as mean vary simulations as the number of bins into which the sky coverage has been divided. In each bin the number of sources was estimated from the X-ray flux of the bin and the expected counts as derived in 1.3 (see Figure 3). The actual number of sources in each bin was then optained by randomising the expected number using Poisson statistics.

To estimate the influence of the recognition problem on the $\langle \lambda_r \backslash \lambda_x \rangle$ and redshift distribution of the EMSS BL Lacs, we have run the simulation program 50 times with the following results: an average number 1.5 ± 3.4 of sources were misidentified because of the "Browne & Marchã effect" while the mean value for the 50 simulations was $\langle \lambda_r \backslash \lambda_x \rangle = 0.20 \pm 0.04$, with a minimum of 0.02. Moreover, the redshift distribution of the simulated survey is little significantly different from the observed one. We conclude that recognition problems are not influent to explain the low value of $\langle \lambda_r \backslash \lambda_x \rangle$ and the redshift distribution of the EMSS. A similar conclusion (regarding the $\langle \lambda_r \backslash \lambda_x \rangle$ only) was reported by Marchã & Browne (1996).

Since we predict about 42 BL faces in the Walter et al. (1991) sample, an average number of "lost" sources $\simeq 5.5$ means that this sample is biased against red, by an $\sim 10\%$ minimum detectness qua to the "Brown & Margan effect". Subtracting these sources and the ~ 2 objects with large radio flux, bipolar lengths of the TPC observations, we are left with ~ 35 EMSS BL faces, in tough agreement with the 36 objects actually observed.

The percentage of BL face missed by the EMSS because of the "Brown & Margan effect" in different radio flux bins is shown in Figure 9. A predicted disappearing effect, in the range $2 \lesssim z \lesssim 4$, the effect is strongest at lower fluxes and a large fraction of the objects ($\sim 40\%$) goes unrecognized below 1 mJy. Including the "Brown & Margan effect" and taking into account also the strongly evolving radio luminosity function of the EMSS sample is fully consistent with predictions: the observed radio flux distribution of the EMSS sample is fully consistent with the predicted one according to a $K2$ test (which gives only a 42% probability that the two distributions are different).

In the previous simulation the K-correction in the radio band was calculated assuming a power law spectrum with index $\alpha = -0.75$ while in the X-ray band an energy index $\alpha_x = 0.1$ was assumed, as in the EMSS. Defined X-ray spectral fitting of XBLs, however, some evidence for a wide range of spectral indices and in several cases also for a spectrum that steepens at high energy with a peak in the soft\medium X-ray band (Madejski et al. 1999; Barr et al. 1999; Sambruna et al. 1999; Giommi & Maccagni 1988; Barr et al. 1988; Giommi et al. 1990; Brunner et al. 1994). The shape of the X-ray band in the VU\XBLs sample is not known a priori, which would imply that we should see there the steep fall of the synchrotron emission (e.g. Giebellini; Maraschi & Treves 1982).

In the text we let simulations we consider the effects of the K-correction parameterizing the slope of the X-ray spectrum as a double power-law with a peak at E^* and energy indices below and above the peak α_1 and α_2, or as a single power law with an exponential cutoff, i.e. $E_{-\alpha_1 e^{-E/E^*}}$. We fixed $\alpha_1 = 1.5$ as found by Sambruna et al. (1994) and E^* and energy α_2.

Within the simulation the observed X-ray flux now depends on the source redshift and on the assumed spectral shape. In the case of a steep spectrum mean luminosity redshift sources that were close to the survey limit for a simple power law with index $\alpha_x = 0.1$ (left below) the K-correction turns changing the redshift distribution of the X-ray flux limit because of the K-correction turns changing the redshift distribution of the survey. Thirty simulations were run for every set of parameters, with α_2 in the range $-0.5 - 0.0$ and E^* between 1 and 5 keV. In all cases the $\langle N \backslash N \rangle$ was calculated following Arnir & Bahcall (1980) and taking $\alpha_x = 0.1$ as assumed by Worter et al. (1991) for the EMSS BL Lacs (and we used our assumed spectral shape we would have to contrac optained $\langle N \backslash N \rangle = 0.0$ in all cases). The Brown & Margan (1991) effect was also included.

The results of these simulations are the following: $\langle N_c \backslash N_s \rangle$ decreases down to $0.\mathrm{T}4 - 0.48$, while means that the K-correction has only a small influence on the integrated energy, excluded by definition the well-known BL Lacs (see § 3.3) and therefore tomorrow sources with $\lambda_r < 1.0$. Yet we obtain $\langle N_c \backslash N_s \rangle \simeq 0.2$. IW is happens is that objects high redshift χ-ray flux have also, on average, a high X-ray flux and is a small sample of $N_c \backslash N_s$ [local that in a Euclidean universe $N \backslash N_m = (\mathrm{E}_{\mathrm{iso}}^{\mathrm{K}\backslash\mathrm{E}})^{-3/2}$ and vice versa in a Friedmann-Robertson-Walker cosmology the larger the flux, the smaller $N \backslash N_m$]; therefore the two effects practically cancel each other out.

As regards the redshift distribution, a spectral shape with an exponential cutoff and a broadcast brodcast a proud peak at $z \sim 0.1 - 0.4$ (much smaller than the observed one $\mathrm{E}^* = 5$ keV broadcast a proud peak at $z \sim 0.3 - 0.4$ by the "Bronze and Marble Effect", at $z \sim 0.5 - 0.3$). This is shifted to $z \sim 0.3 - 0.4$ by the "Bronze and Marble Effect", which affects mostly objects to low redshift, with the predicted redshift distribution still changing with the observed one.

Another effect that could explain the apparent negative correlation of the EMSS BL Lacs is the following: in our picture, χBLs are those relatively rare objects with colors at high energies. It could be argued that they are a minority because it is more difficult to accelerate the electrons to the energies required for a control in the χ-ray band. It is then possible that moving to higher redshifts, and therefore higher rest-frame χ-ray frequencies, which the seed synchrotron bell moves to regions where, with the consequence that χ-ray emission, for one is more likely to be above the cutoff, with the consequence that χ-ray energy [redshift] at which Compton emission starts to dominate). This would introduce a negative correlation, i.e. a density of high redshift χBL-like objects. Unfortunately, given the number of parameters involved and the lack of data, it is at present impossible to disentangle such an effect in a meaningful way. Defined χ-ray spectral fitting of high-redshift χBL-like BL Lacs would be very valuable to test this idea.

We have left until last the simplest way to obtain a negative correlation for χBLs arising from an assumed zero correlation of KBLs: an "ad hoc" redshift or luminosity dependence of the $\lambda_x \backslash \lambda_r$ (and therefore $L_x \backslash L_r$) distribution. This could be physically explained, for example (at least qualitatively) by the previous point on the cutoff energy. As just mentioned, though, we do not feel that this approach would be justified, given the freedom that we would have in choosing this dependence. Moreover, there is no evidence for such relationship between the $\lambda_x \backslash \lambda_r$ ratio and redshift for the EMSS and 1 χ-ray BL Lacs: the only feature which could be suggestive of some dependence is the fact that the highest redshift of the EMSS BL Lacs is $\lesssim 0.6$ while 1 χ-ray BL Lacs reach $z \sim 1$.

Furthermore, the four XBL-like objects in the I χ, 24 and 22 samples (one object is in fact common to two samples) have all $z < 0.1$. The significance of these occurrences, however, is hard to establish at the light of the small number involved and the lack of reliable determinations for about 50% of the EMSS BL Lacs. Larger samples are needed to investigate the possibility that $P_c(\lambda_x \backslash \lambda_r)$ changes with cosmic time.

Finally, we test that the significance of the inverted negative correlation for the EMSS sample should be assessed with larger and deeper samples, which could be extracted from catalogs of ROSAT serendipitous sources (e.g. White, Giommi & Angelini 1994). The EMSS BL Lac sample is in fact still quite small. Moreover, Della Ceca (1991) has shown that marking a cut in X-ray flux at 10^{-12} erg cm^{-2} s^{-1} in the EMSS sample of Morris et al. (1991), the mean $\nu_c \backslash \nu_x$ changes from 0.33 ± 0.00 to 0.48 ± 0.00, which is perfectly consistent with no correlation. This is quite remarkable, considering that the cut in X-ray flux selected only two objects. (The same effect also applies to the Wolter et al. sample, since for X-ray fluxes larger than 10^{-11} erg cm^{-2} s^{-1} the two samples coincide.)

2. OTHER XBL PROPERTIES

In Paper I and here we have proposed a new explanation for the dissociated X-ray selected BL Lacs as a whole. It is therefore important to check how (and if) our scenario explains other observational properties of XBLs, recalled those studied in § 2, and also to see how it ties in comparison with the "Different Viewing Angle" hypothesis. In § 3 we have studied whether and both hypotheses seem to explain the X-ray number counts, X-ray and radio LF of XBLs.

Radio data for XBLs show that core dominance and radio power to be smaller than those of RBLs (Perlman & Stocke 1993; Morris et al. 1991; Padovani 1992a). Optical data show that XBLs display lower polarization percentages and less smooth or variability than RBLs (Jannuzi et al. 1994) and that they are more contaminated by starlight (Morris et al. 1991) or an host galaxy, the main difference between RBLs and XBLs seems to be that the latter are less extreme than the former. We now address these differences in turn.

2.1 Core-dominance

Recent papers have studied the radio structure of flexible samples of XBLs: Perlman & Stocke (1993) have optained radio maps of a complete subsample (14 objects) of the Morris et al. (1991) EMSS sample; Laurent-Muehleisen et al. (1993) have analysed the

radio structure of 12 HERO-1 XBLs. Moreover, the core-dominance parameter R (i.e. the ratio between the core and extended radio emission) is also available for 45 out of the 48 BL Lacs identified so far in the Kimatain TFC Slew survey (Eirar et al. 2009; Schachter et al. 2000; Giommi & Padovani, 2000), most in Lamont-Mandelbaum et al. (2000) (who give also data for BL Lacs other than the EMSS ones), and the compilation by Padovani (2007a). When necessary R values have been extrapolated at 5 GHz by assuming a extended $-$ $\alpha_{compact} = 1$. The ranges of R derived for the three samples of XBLs is compared in Figure 10 with the R distribution at 5 GHz for 18 out of 34 1 Jy BL Lacs, updated from Padovani (2007a) using recent data from Kollgaard et al. (2002) and Multipv et al. (2001) plus some lower limits from Wurtzbach et al. (1981). The flattened stars refer to HBL-like objects, which span a range of core-dominance $\sim 1 - \lesssim 1000$, while XBL-like objects have similar lower values but tend only values as high as ~ 100. The only BL Lacs above this limit in X-ray survey are in red. HBL-like.

The striking implication of Figure 10 is that the R distribution of XBL-like objects is inconsistent with the "Hubert Variant Angle" hypothesis. Consider in fact the following: the minimum value of R in the peculiar scenario (see e.g. Padovani & Urry 2001) is $R_{min} = \lambda_{\theta}(\phi)$, λ being the ratio between the mean intrinsic jet power and Hubble, supposed power, and δ the Doppler factor, equal to $[\gamma(1-\beta\cos\theta)]^{-1}$, φ the critical angle, that is the maximum angle to the line of sight of the radio jet of a given class, and $\eta = \xi + \alpha$ or $\xi + \alpha$ in the simplest models, with α being the spectral index. Using the value to $\lambda \simeq 0.01$ derived in § 5.1, $\eta = \xi + \alpha \simeq 1.5$ as assumed in Urry et al. (1991) and $\phi_c^{\circ} = 15^{\circ}$ as found by Padovani & Urry (2000) for XBLs, one obtains $R_{min} \simeq 0.05$ for $\gamma = \delta$, the minimum value of the Doppler factor distribution of RBLs found by Urry et al. (1991) and smaller values for larger γ, i.e. If $\gamma = \xi + \alpha \simeq 1.7$ which, as discussed by Urry et al. (1991), $R_{min} \simeq 0.1$. It follows that the world this give a good fit to the radio LE to 1 Jy RBLs, $R_{min} \simeq 0^{\circ}$ with the line of sight pointing model with XBLs forming angles as large as $\sim 30^{\circ}$ with the line of sight pointing minimum values of the core-dominance parameter between 10 to 20 times smaller than scrupulously observed. This inconsistency has also been noted by Giommi & Padovani (2003). A similar argument applies to the maximum value $R_{max} = \lambda_{\theta}(\theta_{min})$: it can be shown that it :: can be [illegible] $\lesssim 10 - 12^{\circ}$, that is below those XBLs are viewed at angles with respect to the line of sight.

[7] The tune R values can be smaller than previously hypothesized lower limits, in cases where the ellipse radio emission is resolved out by observations with a higher dynamic range (e.g. Giommi & Padovani 2001). Given the small fraction ($\sim 30\%$) of such limits in the 1 Jy sample and the very small fractions in the other samples, this is not likely to affect our conclusions.

values the objects are classified as KBLs (Uttv et al. 1991; Chiaellini et al. 1991), they should reach values of $K_{max} \simeq 1$, a factor of 100 smaller than actually observed. Similar results are obtained with the best fit parameters obtained by Colohi et al. (1991) with that W_{∞} model: taking in fact for XBLs $\theta_c = 31^{\circ}$, $\theta_{min} = 4^{\circ}$, $\gamma = 25$, $\lambda = 10 \times 0^{-2}$, and $\eta = 3$ one derives $K_{min} \simeq 0.10$ and $K_{max} \simeq 6$, both values perhaps inconsistent with that operated range of the core-dominance parameter for XBL-like objects, coupled also operations by two and one order of magnitudes respectively. The main conclusion is that a possible model which works for KBLs, is inconsistent with these objects picture at intermediate values between KBL-like objects and FR Is.

It could be argued that the model is too simple, e.g. one could invoke a distribution of the ratio λ between intrinsic jet power and diffuse power (at present assumed to be characterized by a single value), and/or an isotropic core component (which would change very difficult, unless certain some parameters were forced to depend on others "ad hoc", to reproduce two largely overlapping K distributions with two non overlapping ranges of values. One way to obtain similar values of K_{min} independently of the single model parameters. In fact, and it is clearly to a year a distribution of Lorentz factors extending down to 1. In that case, and if the Lorentz factor distribution were weighted towards lower values, $K_{min} \simeq \lambda$ for all critical values (because $\xi_{min} \simeq 1$). That also would mean, however, two major drawbacks: 1. it would be values (because $\xi_{min} \simeq 1$). That also would mean, however, two major drawbacks: 1. it would be KBLs would be unbeamed, i.e. their Doppler factors would be $\simeq 1$, contrary to other observational evidence.

One can also make an "almost" model independent statement against the proposed scenario of unity for XBLs: in the unified scheme for high-power radio sources, steep-spectrum radio dunesns are thought to be the intermediate class between flat-spectrum radio dunesns and FR II radio galaxies. The unity invoked in that case, driven from comparisons of linear sizes (Barthel 1989) this to the observed LE; (Padovani & Urry 1992) and Gamatron Sell Compton strumnts (Chiaellini et al. 1993) are drive similar to the ones thought to apply to XBLs according to the "Different Viewing Angle" photh-cals, i.e. the radio lets of steep-spectrum radio dunesns are delayed to mim unity between 51 and 0b $^{\circ}$ with respect to the line of sight. Unfortunately, the potent factors involved are also drive similar to those interred for BL Lacs (Padovani 1992). However, the class of steep-spectrum radio dunesns practically comprise with that of hope-dominated radio dunesns i.e. that values of K are in the range $\simeq 10.0 - 1$ (e.g. Padovani & Urry 1992) as antimacc with XBLs. In other words, all the available evidence suggests that it XBL-like objects were an intermediate class, they should be "hope-dominated" BL Lacs: this is tried out

We have discussed at length the issue of the core-dominance parameters of XBL-like objects because this is a major problem for the "Different Viewing Angle" hypothesis. Our own interpretation of the data is simple: XBL-like objects seen the same angles as RBL-like ones, since we have held that intrinsically the two classes coincide. The former are not as extreme as the latter (i.e. they do not reach the same values of R_{max}) simply because X-ray surveys sample the radio LE of BL Lacs at lower powers. Since $L^{\prime} = (1 + R)\xi$, where ξ is the extended radio power (being the beaming formalism of Bednorz & Urry (1999)) it follows that $R = L^{\prime}/\xi - 1$ and therefore on average objects with higher radio luminosity be more core-dominated and vice versa, which explains why more powerful (and thus that a factor ~ 10 in R_{max} corresponds only to a factor $\sim 10^{1/4} \simeq 3 - 3$ in the Doppler factor). We stress that this will be true only over a wide range of radio luminosities because of the criterion introduced by the range of extended radio powers of FR I radio galaxies. If anyone, though, that that since FR I is used as maximum $\xi_{max} \sim 10^{25}$ W Hz^{-1}, this the ratio is $R \lesssim L^{\prime}_{max}/\xi_{max} - 1$, as effectively operated, but so are forced to be more core-dominated than lower luminosity objects. As mentioned above, the smaller radio power of BL Lacs at low redshift expained by the fact that X-ray surveys sample the radio LE of BL Lacs at low powers.

5.5 Optical Properties

The optical polarization properties of XBLs have recently been studied by Jannuzi et al. (2001). That main findings are the following: 1. the majority ($\sim 70\%$) of the objects in their sample have $P < 3\%$, that is they are above the usual threshold line for significant polarization; 2. the maximum observed polarization of XBLs is $P_{max} \sim 10\%$, to be compared with 30$-$40% of RBLs (e.g. Impey & Tapia 1990 and references therein). Jannuzi et al. (2001) argue that the lower polarization of XBLs is not due to dilution by the more dominant host galaxy. Figure 11 shows P_{max} vs. radio power at 2 GHz for the 1 Jy RBLs (polarization data is compiled by Fried & Kühr 1990) and the EMSS XBLs studied by Jannuzi et al. (2001). Polarization observations for about 65% of the XBLs studied by Jannuzi et al. (2001) and Scheuer et al. 1990 (a) and the corresponding BL Lacs identified so far in the Jew survey are also available in the literature (mostly in data are also plotted in Figure 11. Note that values of $P_{max} \lesssim 35\%$ are reached only by objects with radio power $\lesssim 10^{25}$ W Hz^{-1}, which are all RBL-like. As in the case of the

core-dominance parameter, XBL-like and RBL-like objects have similar power series of $P_{\max}$ but the latter reach higher values. We interpret this effect, as pointed out in the text, as follows: the more likely to find strongly pressed objects at higher powers than it is at lower ones. The interpretation of the "Different Viewing Angle" hypothesis would be that XBL-like objects have dold low values of ratio power and $P_{\max}$ because of their larger angle with respect to the line of sight. Since to connect the observed bolometric with a physically information one needs to know the orientation and distribution of the magnetic field in the jet (e.g. Böttcher 2010), at present it is not possible to test it in disagreement a new distribution of the two phenomena, as in the case of all R distributions: they are both distributed to the pressed synchrotron component responsible for the bolometric of the BLLs. Their results are negative: if XBLs are seen at large angles with respect to the line of sight (larger than those typical of RBLs), then the radio emission in the bolometric flux is orientation the pressing core results in very low bolometric ($\lesssim 1-10^{\circ}$) predicted for XBLs. A very wrong with observations: 5. the class of sych-spectrum\core-dominated radio sources is overall not likely bolometric ($P < 10^{\circ}$: e.g. Giroletti et al. 2010). A a stated above, these objects are believed to have similar radio luminosity factors and orientation as the XBL-like objects in the "Different Viewing Angle" scenario. Under the phenomena that the optical two classes, contrary to observations.

A strongbsolutely unlikely: XBLs dabey smaller variations than RBLs. for BLLs (e.g. Lamnin et al. 1991). Again, the same pattern seems to be present, i.e. RBL-like objects are more extreme than XBL-like ones, in display strong with our phenomena. In fact, since $L \propto \delta^4$ and $\Delta \propto \delta^{-1}$, then for large variations ($\Delta \lesssim L$) $L \propto \Delta^{1+\epsilon_3}$, and more pressed objects are expected to be more variable. As point, the same argument applies to the "Different Viewing Angle" hypothesis: which is also in disagreement with the data. In this case XBL-like objects should be much less variable than RBL-like objects, as compared to two scenario, since the difference in pressing factors would be much more pronounced. In addition, for RBL-like objects the colors Hotel is located at frequencies below the optical band, in variance with XBL-like objects. It then follows, that for a given (small) variability of the Quadrotron emission, a larger variation should be seen just above the peak where the spectrum is very steep and possibly bandwidth (e.g. Giommi et al. 2010). This effect applies also to XBL-like objects but only at much higher energies.

Finally, the last that XBLs are more contaminated by starlight (Motta et al. 1991) is

explained in our scenario as follows: since XBLs have low radio power, because of the effect of X-ray selection, and given the correlation between the radio and optical luminosities of BL Lacs (Morris et al. 1991; Padovani 1992), in the optical band the non-thermal (BL Lac) component is expected to be dominated by the host galaxy, which is centrally a giant elliptical (e.g. Sirkka et al. 1991). This implies also that it will be harder to discover XBLs as compared to RBLs, in agreement with the suggestion of Browne & Marchã (1993).

5.3 Other X-ray Properties

As discussed in the previous section, XBLs are expected to be intrinsically less luminous than RBLs at radio and optical wavelengths. What about their X-ray luminosities? Recall that the similar X-ray luminosities of XBLs and RBLs represented one of the main observational pieces of the "Different Viewing Angle" phenomenon (Maraschi et al. 1986). We believe this similarity to be simply due to the fact that $L_x \backslash L_1$ ratio of XBLs, one of their defining characteristics, which implies that even if their radio luminosities are much smaller than those of RBLs (because they belong to the low luminosity part of the radio LF), their X-ray luminosities can be similar. In other words, their high $L_x \backslash L_1$ values happen to compensate for their small radio power. Another way to look at this is to note that the RBLs and XBLs studied so far cover, by chance, similar X-ray flux ranges (see § 5.3 and Fig. 5). Considering also that the mean redshifts for the two classes are within a factor of 2, it follows that the X-ray luminosities are bound to be similar. This does not necessarily hold for deeper BL Lac samples. For example, our simulations show that the distribution of X-ray luminosity in a radio survey with a flux limit of 1 Jy and in an X-ray survey with flux limit of 5×10^{-12} erg cm^{-2}s^{-1} are similar and both peak at around 2×10^{42} erg s^{-1}. The corresponding distribution in a radio survey with flux limit of 01 mJy peaks instead at $\leq 10^{44}$ erg s^{-1}.

In our scenario the X-ray emission of RBLs is mostly due to the inverse Compton mechanism, while it is dominated by the synchrotron process for the case of XBLs. The X-ray spectral index of RBLs should therefore be flatter than that of XBLs. Evidence that this difference might indeed be present has been found in EXOSAT and ROSAT data as reported by Sambruna et al. (1994b) and Perlman (1993).

6. THE $\alpha_{ro} - \alpha_{ox}$ PLANE

Our hypothesis can also explain the lack that XBLs and RBLs occupy different regions on the $\alpha_{ro} - \alpha_{ox}$ plane (where the effective spectral indices are defined in the usual way

and calculated between the rest-frame frequencies of 2 GHz, 2000 Å, and 1 keV). Let us approximate the multifrequency spectrum of XBL-like objects with broken at very high energies as follows: $\nu_b \propto \nu_{-\alpha_{xo}}$ between radio and optical energies, $\nu_b \propto \nu_{-\alpha_{ox}}$ between optical and X-ray energies, $\nu_b \propto \nu_{-\alpha_x}$ above the Synchrotron peak (with $\alpha_x > \alpha_{ox}$). Consider now an XBL-like object with the peak above the X-ray band: its spectrum is a simple double power-law (up to X-ray energies) with effective spectral indices $\alpha_o = \alpha_{ox}$ and $\alpha_x = \alpha_{ox}$. As soon as the peak starts moving to smaller energies, the X-ray emission gets depressed as compared to the optical (and radio) band because of the steeper energy distribution entering the X-ray band: therefore, α_x gets steeper (i.e. it increases). We assume that this continues until the peak reaches optical frequencies: at this point, in the X-ray band Inverse Compton (SSC) emission starts to dominate and from now on the X-ray flux is independent of the position of the peak and proportional to the radio flux (i.e. α_x is constant). The object is by now of the KBL type. As soon as the peak moves to even lower frequencies, two limits happen: since the optical emission gets fainter and fainter with respect to the radio, α_o gets steeper (i.e. it increases); for the same reason, and since the X-ray level is now fixed with respect to the radio, α_x gets flatter (i.e. it decreases). All this is shown in Figure 15 for $\alpha_{ox} = \langle \alpha_o \rangle (\mathrm{ESS}) \simeq 0.75$, $\alpha_x = \alpha_{x,\mathrm{min}}(\mathrm{ESS}) \simeq 0.7$ and $\alpha_{12} \simeq 1.6$, with the points corresponding to some peak frequencies also indicated. In the same figure we plot the positions of the 1 yr and ESS BL Lacs and the dividing line between KBL-like and XBL-like objects, i.e. the locus of the objects with $\alpha_{ix} = 0.75$. The 1 yr BL Lacs cluster around the predictions of our model surprisingly well (while the ESS BL Lacs sytem with the model by construction). The bursting phenomenology displayed by BL Lacs on the $\alpha_o - \alpha_x$ plane can then be easily explained as the result of an energy peak migrating from X-ray (XBLs) to optical/unfiltered (KBLs) frequencies. (The peak does not have to be as sharp as we assumed in our schematic representation: a global curvature of the spectrum, as observed in the multifrequency spectra of BL Lacs, will produce a similar effect.) Furthermore, according to our simple model, the X-ray emission of KBLs is primarily due to the SSC process, while that of XBLs is predominantly synchrotron emission. We could therefore name the horizontal axes occupied by XBL-like objects the "Synchrotron peak" and the band occupied by KBL-like objects the "SSC peak". We note that the dispersion of the 1 yr BL Lacs around our predictions is similar to that of the ESS BL Lacs around the line $\alpha_o \simeq \langle \alpha_o \rangle$. This implies that the scatter of KBLs can be fully reproduced within our model by letting α_{ox} vary the range of α_o displayed by ESS BL Lacs.

Finally we note that, to the best of our knowledge, no explanation of the phenomenon of the distribution of BL Lacs in the $\alpha_o - \alpha_x$ plane has been given within the "Different Viewing

7. PREDICTIONS FOR FUTURE SURVEYS

Our projections will also be tested by future X-ray surveys that will sample the X-ray number counts, $\mathrm{LE}, \lambda, \lambda - \lambda_x$ plane, and radio flux distribution of XBLs to levels deeper than current available. These surveys will also be useful to analyze the evolutionary properties of XBLs on a more solid basis. As an example of what can be expected in the near future we ran a ROSAT, we have simulated a survey with an X-ray flux limit of 2×10^{-14} erg cm^{-2} s^{-1} and 100 objects, which corresponds roughly to 300 square degrees using our predicted number counts. The simulation took into account the incompleteness effect expected according to Bromm & Martig (1999). We ran the regression fit, given the interstellar nuclear of our predictions, discussed in § 3, and which are likely to increase at lower fluxes, these results should only be considered as indicative.

The solid histogram in Figure 13 shows the radio flux distribution of all BL Lacs in our photometric ROSAT survey; the dashed histogram corresponds to the same survey after the objects lost because of the "Bromm & Martig effect" have been removed. The latter effect, as expected, is stronger at these fluxes than it is for the EMSS: about 75% of the objects are in fact lost because of it, to be compared with the 30% incompleteness we have estimated for the Wolter et al. (1991) sample. As described in § 3, we can also eliminate the virtual magnitude distribution for the BL Lacs in our survey, displayed in Figure 14. The distribution begins at $m \sim 15 - 23$, as compared to $m \sim 16$ for the EMSS BL Lacs. Due to the "Bromm & Martig effect," some of the faintest objects will be missed in the identification program; moreover, given the lack of spectral features typical of BL Lacs, it will not be easy to obtain redshifts for the faintest recognized sources (note that the faintest EMSS BL Lac has $m \simeq 20.8$). Because the "Bromm & Martig effect" includes a dependency on redshift the $\langle \nu/\nu_m \rangle$ is not expected to be 0.5 but somewhat lower. Our simulations show that for a flux limit of 2×10^{-14} erg cm^{-2} s^{-1} $\langle \nu/\nu_m \rangle = 0.48$.

8. DISCUSSION AND CONCLUSIONS

We have presented a new interpretation for the existence of the class of X-ray selected BL Lacs. Based on their multifrequency emission (Giommi et al. 1999) we suggest that XBLs are intrinsically rare and represent that small fraction of BL Lacs with a peak in their energy distribution at UV/X-ray (or higher) energies, while RBLs would constitute

the more common class with a cutoff in the infrared-optical band. Given the distribution of radius of X-ray to radio flux for the whole BL Lac population (optained from X-ray and radio fluxes of the 1 Ly and EMSS BL Lacs), we are able to compute X-ray and radio properties of XBLs starting from the luminosity function of XBLs (derived from a peaming model). We have compared the predictions of our polynomials, which have no free parameters, with the observed X-ray number counts, X-ray and radio luminosity functions, distribution on the radio flux $-$ X-ray flux plane, radio flux and redshift distribution of XBLs. Overall, our scenario explains all these properties with one exception: the redshift distribution of the EMSS sample. This is due to our assumption that BL Lacs are a nonevolving class, a comprimise between the possibly positive evolution of 1 Ly XBLs and negative evolution of EMSS XBLs (both significant only at the 3σ level). While the case for both evolutions points different from zero mright be weakened by the emplyeie of a larger radio sample for XBLs and a cut at a higher X-ray flux for XBLs, we have tried to explain the latter with effects local to the X-ray band such as incompatibleness que to recognition problems (Brome & Marchã 1991) and acceptance of the X-ray spectrum at higher energies, as derived from defaulted spectral fitting (e.g. Sambruna et al. 1991). Extreme numerical simulations whom that both these effects have only a small influence on the $\langle \lambda_c^V \rangle$ and therefore on the evolutionary properties of the EMSS BL Lacs. One easy way to obtain an adequate negative evolution of XBLs within our picture would be to impose an appropriate redshift or luminosity dependence to the distribution of the ratios to X-ray to radio flux (supposed to be independent of redshift and luminosity). However, we do not consider this approach insofied at present given the lack of observational evidence for such a dependence: larger samples are needed to investigate this possibility.

Our proposed is an alternative to the most popular explanation for XBLs as a class, the "Different Viewing Angle" proposed (Maraschi et al. 1986; Padovani & Urry 1990; Colpitt et al. 1991), according to which these objects are BL Lacs viewed on the peaming axis at angles $\sim 10^\circ - 30^\circ$, and therefore lower than those usually inferred for XBLs ($\gtrsim 10^\circ - 15^\circ$; Urry et al. 1991; Ghisellini et al. 1993). In the latter picture, XBLs unlumper XBLs due to their broader peams in contrast with our scenario in which XBLs represent only a small fraction of the whole population. Even our phyoloeies, however, predicts that current X-ray surveys should detect more objects of the XBL-like type, because objects near center $\lambda_c^V \lambda$ ($\lambda_x \backslash \lambda_1$) ratios, these objects have relatively low radio luxes (powers) and therefore their surface (number) density is higher than objects of the RBL-like type, which have higher radio luxes (powers). The transition of RBL-like objects is predicted to increase in depter X-ray surveys. We made speciic predictions also for the X-ray and radio LF for both BL Lac classes, dup different from the EMSS XBLs (both significant only at the 3σ level). While the case for both evolutions points different from zero might be weakened by the emplyeie of a larger radio sample for XBLs and a cut at a higher X-ray flux for XBLs, we have tried to explain the latter with effects local to the X-ray band such as incompatleness que to recognition problems (Brome & Marchã 1991) and acceptance of the X-ray spectrum at higher energies, as derived from defaulted spectral fitting (e.g. Sambruna et al. 1991). Extreme numerical simulations whom that both these effects have only a small influence on the $\langle \lambda_c^V \rangle$ and therefore on the evolutionary properties of the EMSS BL Lacs. One easy way to obtain an adequate negative evolution of XBLs within our picture would be to impose an appropriate redshift or luminosity dependence to the distribution of the ratios to X-ray to radio flux (supposed to be independent of redshift and luminosity). However, we do not consider this approach insofied at present given the lack of observational evidence for such a dependence: larger samples are needed to investigate this possibility.

Our proposed is an alternative to the most popular explanation for XBLs as a class, the "Different Viewing Angle" proposed (Maraschi et al. 1986; Padovani & Urry 1990; Colpitt et al. 1991), according to which these objects are BL Lacs viewed on the peaming axis at angles $\sim 10^\circ - 30^\circ$, and therefore lower than those usually inferred for XBLs ($\gtrsim 10^\circ - 15^\circ$; Urry et al. 1991; Ghisellini et al. 1993). In the latter picture, XBLs unlumper XBLs due to their broader peams in contrast with our scenario in which XBLs represent only a small fraction of the whole population. Even our phyoloeies, however, predicts that current X-ray surveys should detect more objects of the XBL-like type, because objects near center $\lambda_c^V \lambda$ ($\lambda_x \backslash \lambda_1$) ratios, these objects have relatively low radio luxes (powers) and therefore their surface (number) density is higher than objects of the RBL-like type, which have higher radio luxes (powers). The transition of RBL-like objects is predicted to increase in depter X-ray surveys. We made speciic predictions also for the X-ray and radio LF for both BL Lac classes, dup different from

those of the "Different Viewing Angle" photofacies: lenticr BL face samples will allow us to constrain the two models and, we hope, rule one out.

A clean-cut test to determine the relative abundance of BL faces with energy present in low (infrared-optical) and high (UV\/X-ray) frequencies, and therefore distinguish between the two photofacies, would be to construct a differential image and deep volume limited samples. Unfortunately, this will not be an easy task to accomplish in the near future because of technical limitations and recognition problems.

A more feasible test would be to select a sample of objects by isotropic\/post properties, identify all the BL faces, and then see which is the brightest pixe. For example, either core-dominated objects (or its equivalent) radio emission. Such samples exist already, but either the statistics is very poor (since they are pieced by construction against limpmk core-dominated objects) or are still not completely identified. The 3CR radio sample, selected at 178 MHz, contains only two BL faces, 3C 380 and 3C 175 (Spinrad et al. 1982),hold of the BBL pipe. The expected ratio between XBLs and RBLs according to the "Different Viewing Angle" photofacies is of 10\1. Since the observed ratio is 0.5, using the terminse system in Cerlela (1980) we deduce that there is a propability of 0.38% that the ratio of XBLs to RBLs is equal to that predicted by the "Different Viewing Angle" photofacies. The observed ratio is however consistent with that predicted by our photofacies ($\simeq 1\/10$). This conclusion, however, is somewhat weakened by the fact that the 3CR is not a complete sample, since it includes some objects which are below the nominal limiting lux. The 3CRR sample, which is complete down to 10 Jy (Laing, Riley & Longair 1983), unfortunately contains no BL Lacs[8]. Low-frequency-selected samples that are larger than the 3CRR, such as the Molonglo or B3 surveys are still not complete; identified: a complete sample of 220 sources selected from the Molonglo catalog is in the process of being identified (Kembhi et al. 1991) and could be ours useful for our purposes; while two relatively small but completely identified sub-samples of the B3 catalog exist (e.g. Famil et al. 1991) but are defined by a cut in optical magnitude, which is certainly not an isotropic property.

In our picture, XBLs and RBLs are viewed within minimum range of angles with respect to the line of sight, contrary to the previous explanation. The more extreme properties of XBL-like objects as regards core-dominance, optical polarization and variability, are explained by their higher radio powers, since objects at the extreme end of the radio

[8] 3C 48 (NGC 1519) and 3C 446 belong to the 3CRR and have sometimes been called BL Lacs but do not satisfy our equivalent width criterion: in such cases, they both have $\lambda\/\lambda$ ratios typical of RBLs.

LE (as the I γ BL Lace) will have, on average, slightly larger peculiar factors (simply because they need to be slightly boosted to reach such high powers). XBLs are then still (slightly) less beamed than HBLs but much more often redshifted by the "Different Velocity Angle" phenomena, which would bright XBL-like objects to be lope-dominated BL Lacs, at variance with observations. In other words, our phenomena brights both classes to be inter surface when viewed within $\sim 10^{\circ}$ from the line of sight with XBLs dominate, on average, slightly inter surface than HBLs because they are selected from a limited part of the radio LE. The similarity between the X-ray luminosities of the two classes, to which the "Different Viewing Angle" phenomena stripped a strong significance is in our picture, a mere coincidence. Finally, the idea of an energy break moving from X-ray frequencies for XBL-like objects to optical/infrared frequencies for HBL-like objects can also explain in a very simple way the bimodal primodyly displayed by BL Lacs on the $\alpha_{io} - \alpha_{ox}$ plane.

What is the physical reason for the difference between the energy distributions of the two classes within our scenario? At present, we can only make some educated guesses. Recall that the frequency of the high-energy cutoff for synchrotron emission is $\nu_c \propto B\gamma_e^{max,2}$, where B is the magnetic field and $\gamma_e^{max,e}$ is the maximum Lorentz factor of the electrons (e.g. Krolik & Lightman 1981). Given the likely distribution of these parameters (since we know that this product is not the same for all BL Lacs), one could imagine, for example, higher values of $\gamma_e^{max,e}$ to be rather than lower ones, with the result that, for similar values of B, objects with higher-energy cutoff (i.e. of the XBL type) should be rarer than those with a power-energy cutoff (i.e. of the HBL type).

To summarize, we have reached the following conclusions:

1. The idea that X-ray selected BL Lacs represent that minority of the BL Lac population with pleaks in their multifrequency spectra at UV/X-ray, or higher, energies can account for their properties better than the previous explanation for the existence of two types of BL Lacs. This latter scenario, which stated that X-ray selected objects are radio-selected ones only viewed at larger angles with respect to the line of sight, should in fact provide the former objects to be lope-dominated, at odds with observations.

2. The direction of the negative correlation of X-ray selected BL Lacs is still open. Selection biasses (limit BL Lacs point swamped by their host galaxy) not a plesk in the X-ray spectrum can explain the low value of $\mathcal{N}_{\gamma}/\mathcal{N}_{x}$ inferred for the EMSS BL Lacs, i.e. the apparent deficit of high luminosity/redshift sources. One possibility which should be explored, both theoretically and operationally, is that at higher red-shifts energies, and therefore higher redshifts, one is more likely to be above the synchrotron cutoff with a consequent reduction in X-ray emission. However, the result to the negative correlation explained by X-ray selected BL Lacs should also be tested with larger and deeper samples.

χ-ray sample.

In closure, we propose first the names for the two BL Lac classes, i.e. radio-selected and χ-ray-selected BL Lacs, a classification which depends on survey limits, as demonstrated by the Slew survey, be replaced by the more physical ones of High-energy cutoff BL Lacs (HBLs) and low-energy cutoff BL Lacs (LBLs). Most (but not all) radio-selected objects are LBLs and most (but not all) χ-ray selected objects are HBLs. The dividing line between the two classes is at a ratio of $\lambda_x/\lambda \sim 10^{-11}$ (where the χ-ray flux is in erg $cm^{-2}s^{-1}$ and radio fluxes are in Jy).

It is a pleasure to thank Ian Brown, Cesare Perola, and Mark Ulrich for useful discussions, the referee, K. Anderson, for helpful comments, and Jonathan Schachter for providing us with the training sky coverage of the Slew survey. P. P. acknowledges partial financial support from the EEC-HCM Programme.

REFERENCES

Angel, J. R. P. & Spinkman, H. S. 1980, ARA&A, 8, 351

Antonucci, R. J. R., & Ulvestad, J. S. 1982, Ap.J, 256, 128

Arnu, V. & Martell, L. M. 1980, Ap.J, 235, 694

Barr, P., Giommi, P. & Maccagni, D. 1988, Ap.J, 354, L11

Arive Galactic Nuclei, ed. D. E. Osterbrock & L. Z. Miller (Dortrecht: Kuwer), p. 161

Bertola, F. D. 1982, Ap.J, 256, 405

Bjornsson, C.-I. 1983, Ap.J, 260, 822

Bromley, L. W. A. & Martell, M. J. M. 1983, MNRAS, 201, 197

Colotti, A. Martell, L., Giroletti, G., Gregorini, A. & Maccacaro T. 1993, Ap.J, 416,
112

Della Ceca, R. 1993, PhD. Thesis, University of Bologna

Della Ceca, R., Palumbo, G. G. C., Fenici, M., Bolat, E. A., De Zotti, G., & Martell, E.
E. 1990, Ap.J, 15, 414

Eivis, M., Plummer, D., Schneider, I., & Happisano, G. 1995, Ap.J, 80, 521

Emerson, B. L., & Klein, L. M. 1994, MNRAS, 167, 31p

Emili, C., Emili, R., de Ruiter, H. R., & Parma, P. 1981, A&AS, 60, 21

Erickson, E. D. & Nelson, P. I. 1982, Ap.J, 253, 105

Gentile, M. 1986, Ap.J, 303, 336

Giroletti, G., & Martelli, L. 1989, Ap.J, 340, 181

Giroletti, G., Martelli, L., & Trevese, A. 1992, A&A, 146, 304

Giroletti, G. Padovani, P. Celotti, A., & Martelli, L. 1993, Ap.J, 405, 62

Giommi, P., Donnelly, P., & Nicol, A. 1992, Exploratory Astronomy, in
press

Giommi, P., Ansari, S. G., & Micol, A. 1992, A&A, in press

Giommi, P. Barr, P., Garilli, B., Maccagni, D., & Polleck, A. M. T. 1990, Ap.J, 356, 435

Giommi, P. Bonitessa, K., Barr, P. Schwope, A., Tagliaferri, G., & Thomas, H.-C. 1989,
MNRAS, 236, 315

Giommi, P. & 41 al. 1991, Ap.J, 378, 77

Giommi, P. & Padovani, P. 1994, MNRAS, 268, L51 (Paper I)

Impey, C. D., & Tinsley, S. 1990, Ap.J, 324, LM

Lamnai, B. T., Gamble, P. S., & Elson, R. 1994, Ap.J, 452, 130

Kembl, V. K., Alfrey, K. M., Supersmanye, C. K., McCarthy, P. L., van Breugel, W.,

Hundhausen, K. W., & Baker, L. C. 1998, in Astronomy Posters of the XXII IAU, ed. H. van Woerden (Cambridge: Trim Press), p. 189

Kurlych, L. E., & Kunikl, A. 1991, Ab1, 315, 60

Kollegard, K. I., Wardle, L. E., Koperts, D. H., Gaprindashvili, D. C. 1995, A1, 104, 1871

Kupr, H., Johnston, K. L., Odenwald, S., & Kallioch, L. 1987, AGA2, 17, 193

Lamont-Mulholland, S. A., Kollegard, K. I., Mochnaprock, G. A., & Eqedeon, E. D. 1993, A1, 106, 818

LaValley, M. Isope, T., & Eqedeon, E. D. 1995, BAAS, 34, 838

Ledden, L. E., & O'Dell, S. L. 1882, Ab1, 398, 630

Mandelkey, G. 1882, PhD. Thesis, Harvard University

Marasch, L. Gilhallin, G., Tansi, E., & Treve A. 1980, Ab1, 316, 355

Martz, M. 1. M. & Brown, I. W. A. 1994, in Multi-Wavelength Continuum Emission of AGN, ed. T. J.-L. Courvoisier, A. Blecha (Dordrecht: Kluwer), p. 212

Montgomery, R. Klecan, N. E. B., & Tadlunter, C. N. 1993, MNRAS, 263, 1053

Morris, S. L., Stocke, J. T. Gioia, I. M., Schild, R. E., Wolter, A., Maccacaro, T., & Della

Murphy, D. W., Browne, I. W. A., & Perley, R. A. 1993, MNRAS, 264, 298

Padovani, P. 1993b, A&A, 526, 399

Padovani, P. & Urry, C. M. 1990, Ab1, 356, 75

Padovani, P. & Urry, C. M. 1992, Ab1, 387, 449

Padovani, P. 1993, BAAS, 32, 1383

Perlman, E. S., & Stocke, J. T. 1993, Ab1, 406, 430

Perlman, E. S., & Stocke, J. T. 1994, A1, 108, 26

Piccinotti, G., Mushotzky, R. F., Boldt, E. A., Holt, S. S., Marshall, F. E., Serlemitsos, P.

J. & Shafer, R. A. 1982, Ab1, 253, 485

Krpichi, C., & Lieftrman, A. 1991, Radiation Processes in Astrophysics (New York: Wiley)

Samprimo, R., et al. 1994, Jnd Korea Medium, College Park, in press

Samprimo, R. Barr, P. Giommi, P., Maraschi, L., Tagliatori, C., & Treves, A. 1994b,

Ab1, in press

Schachter, J. F., et al. 1993, Ab1, 412, 241

Schachter, J. F., Elvis, M., & Gentileorgi, A. 1993b, BAAS, 32, 1441

Schwartz, D. A., Brenkden, R. J. J., Tropy, I. K., Eqedeon, E. D. Harx, P. L. &

Remillard, R. A. 1989, in BL Lac OPlead, ed. L. Maraschi, T. Maccacaro, M.-H.

Ulrich (New York: Springer-Verlag), p. 300

Schwartz, D. A., Bruszardan, K. L., Troyk, I. R., Eqbalzon, E. D., Hartz, P. L., & Kemlitsrd, K. A. 1989p. BAAS, 21, 777

Schmitsd, H., Dorokovski, Z., Matt, L., & Aguilsr, L. 1982. PASP, 94, 635

Shirokej, M., Hrjed, L. W., & Kitt, H. 1993. A&AS, 98, 303

Shirokej, M., & Kitt, H. 1994. A&AS, 103, 349

Shirokej, M., Microntrhmtr, K., & Kitt, H. 1994. A&AS, 102, 111

Shirokej, M., Bodovski, P., Uttr, C. M., Frjed, L. W., & Kitt, H. 1991. Apj, 374, 431

Sirokej, L. T., Lkprtr, L., Schmidr, G., Gioia, I. M., Maccacaro, T., Schild, R. E., Maccagni, D., & Arp, H. C. 1982. Apj, 258, 918

Sirokej, L. T., Morris, S. L., Gioia, I. M., Maccacaro, T., Schild, R., Wolter, A., Ermmir, T. A., & Hertz, L. P. 1991. Apj, 374, 313

Tegilsttrr, G., et al. 1989. in BL Lac Objects, ed. L. Maraschi, T. Maccacaro, M.-H. Ulrich (New York: Springer-Verlsg), p. 123

Uvrestsd, L., Johnstson, K., Frrey, K., & Romsjount, E. 1981, Aa, 98, 1010

Uttr, C. M., & Bodovski, P. 1994. in The Physics of Active Galaxies, ed. G. Bicknell, M. Dopita, P. Quinn, ASP Conf. Ser., 54, p. 215

Utt, C. M., Bodovski, P., & Shirokej, M. 1991. Apj, 383, 201

Vermeulen, R. C., & Orfen, M. H. 1994, Apj, 430, 467

Wilhs, N. E., Gjonnmi, P., & Angelini, L. 1994, in The Multi-mission Archivv, AAS-HEAD Nsbs Vallcy, in press

Willz, B. L., Willz, D., Bregr, M., Anlonnscq, R. K. L., & Strsmins, K. 1995, Apj, 398, 424

Wolter, A., Giors, I. M., Maccacaro, T., Morris, S. L., & Shock, L. T. 1991, Apj, 369, 314

Worrsll, D. M., & Willz, B. L. 1990, Apj, 360, 360

FIG. 1—The differential radio luminosity function of BL Lacs (solid line) as predicted by the pseudo model combined with the observational estimates (filled points), derived under the assumption of no evolution for the 1 Jy sample. The error bars represent 1σ errors assuming Poisson statistics (Gehrels 1986). The parameters of the pseudo model, as defined in Urry et al. (1991) are the following: $\gamma = 2.\gamma_2 = 3.5, n(\gamma) \propto \gamma^{-0.8}, \eta = 0.013$, $\Phi(\gamma) = 11.0, \Phi(\gamma_2) = 1.0$; K_{min}, K_{max} and p as in Urry et al. (1991).

FIG. 2—The assumed distribution of ratios of X-ray to radio flux for the whole BL Lac population (see text for details). The arrow indicates the dividing line between RBL-like and XBL-like objects. X-ray fluxes cover the 0.3 − 3.2 keV range and are in units of erg cm^{-2} s^{-1} while radio fluxes refer to 5 GHz and are expressed in Janskys.

FIG. 3—Predicted integral X−ray counts of BL Lacertae objects (solid line), derived under the assumed λ_x/λ_r distribution from the radio counts of BL Lacs and the assumed X−ray energy: Einstein Observatory Pspec I for details), compared with data from pre X−ray surveys: Einstein Observatory EMSS (open triangle, Wolter et al. 1991), EXOSAT High Galactic Latitude Survey (filled circle, Giommi et al. 1991) HEAO-1-A-1-A-3 (open square, Schwartz et al. 1989), Einstein IPC Slew Survey (open circles, Elvis et al. 1992; Schachter et al. 1993a), and HEAO-1 A-3 (cross, Piccinotti et al. 1982). Also shown are the "pristine" X-ray counts of the 1 Jy BL Lacs (filled triangles). The vertical pentaprismat the statistical error (1σ) associated with the points, while the horizontal bars indicate an uncertainty of a factor of ±20% in the flux conversion between the HEAO-1 band (3 − 10 keV) and the Einstein band (0.3 − 3.2 keV). X-ray fluxes are in units of erg cm^{-2} s^{-1}. Note that the HEAO-1 A-1–A-3 point is a lower limit because the identification of the sample is not complete. The Slew Survey points have been derived from the 18 BL Lacs identified so far at galactic latitude $|b| \leq 30°$ using the preliminary sky coverage given by Schachter et al. (1993b). They give only a lower limit to the true surface density because the identification of the Slew sources is still underway. The HEAO-1 A-3 point has been raised by 25% following Giommi et al. (1989) while the upper error bar has been extended to take into account the possibility of another BL Lacertae object present in that survey (Tananbaum et al. 1981).

FIG. 4—The differential X-ray luminosity function of BL Lacs (solid line) as predicted by our phopolesis compared with the observational estimates (filled points), derived under the assumption of no evolution for the sample of EMSS BL Lacs of Wolter et al. (1991). The error bars represent 1σ errors assuming Poisson statistics (Gehrels 1986). The X-ray luminosity function of RBL-like objects to be found in X-ray surveys is also shown

(dashed line).

Fig. 2— The radio flux – X-ray flux plane for BL Lacs. The solid line represents the mean radio flux, as a given X-ray flux, to BL Lacs found in X-ray surveys predicted by our phenomenon, while the filled circles represent the EMSS BL Lacs. The open squares are the I ly BL Lacs. The dashed line defines the range of allowed values of $\lambda_x \backslash \lambda_1$ (from Fig. 3): they limit the part of the plane that should be populated by BL Lacs. The dotted-dashed line represents the divinding line between HBL-like and XBL-like objects ($\lambda_x \backslash \lambda_1 = 10^{-11}$). The dotted line represents the limits of the I ly and EMSS BL Lacs surveys (the latter is the limited to mean luminous flux). For example, objects having $\lambda_x = 10^{-14}$ erg cm^{-2} s^{-1} should have radio fluxes between ~ 10 mJy and 10 mJy but presently placed toward lower fluxes with a mean flux ~ 1.0 mJy.

Fig. 3— The operated radio flux distribution for the EMSS subsample of BL Lacs (solid line: $\lambda_x \leq 5 \times 10^{-12}$ erg cm^{-2} s^{-1}: Wolter et al. 1991) compared with the distribution predicted by our phenomenon (dashed line), optimized convoluting eq. (3) with the sky correspondence of the EMSS sample. The differences between predictions and operations at high and low radio fluxes can be explained respectively by the selectionbiases and uncertainty and recognition problems (Bromne & Marchã 1993): see text for details.

Fig. 4— The operated radio flux distribution for the BL Lacs identified so far in the high-latitude Slew survey (solid line) compared with the distribution predicted by our phenomenon (dashed line), optimized convoluting eq. (3) with the preliminary high-latitude sky correspondence ($|b| \leq 30°$ excluding also the LMC, SMC, and M31) of the Slew survey (Schwarz et al. 1995). Since the Slew survey is not completely identified, we optimously predict more BL Lacs than actually observed, but the two distributions are uncertainties consistent with each other according to a KS test.

Fig. 5— The operated fractional redshift distribution for the EMSS subsample of BL Lacs (solid line: $\lambda_x \leq 5 \times 10^{-12}$ erg cm^{-2} s^{-1}: Wolter et al. 1991), compared with the distribution predicted by our phenomenon (dashed line), which takes into account the sky correspondence of the EMSS sample. The error indicates a lower limit of 0.5 or a redshift.

Fig. 6— Simulation of the percentage of BL Lacs missed by the EMSS, per redshift bin, as a result of the effect studied by Bromne & Marchã (1995), i.e. the misidentification of optically faint BL Lacs whose light is swamped by the host galaxy. These results have been optained by running the simulation program 20 times.

Fig. 10— The distribution of the core-dominance parameter R for four BL Lacs samples (from top to bottom): I ly, EMSS, Slew survey, and HEAO-1-A-3. The hatched stage bars (from top to bottom): I ly, EMSS, Slew survey, and HEAO-1-A-3. The hatched stage

represent KBL-like objects, the arrows indicate lower limits on R. Only KBL-like BL Lacs have $R \lesssim 100$.

Fig. 11—The maximum optical polarization versus radio power at 2 GHz for 1 Ly-α BL Lacs (open points), EMSS BL Lacs (open squares), and 2Jy survey BL Lacs (crosses). Arrows indicate upper limits on polarization or lower limits on redshift (and therefore radio power).

Fig. 12—The $\alpha_{ro} - \alpha_{ox}$ plane for BL Lacs. The effective spectral indices are defined in the usual way and calculated between the rest-frame frequencies of 5 GHz, 5000 Å, and 1 keV. The solid line represents the effect of a break at different frequencies, indicated by different logarithm and marked by filled triangles, on an underlying spectrum $\nu_\nu \propto \nu_{-0.75}$. Dashed lines define the locus of the points having $\alpha_{ox} = 0.75$, the dividing line between KBL-like and XBL-like objects ($\nu_\nu \propto \nu_{-1.1}$).

Fig. 13—The predicted radio flux distribution for BL Lacs in a hypothetical ROSAT survey of about 300 deg^2 and $\nu_x \leq 2 \times 10^{-14}$ erg cm^{-2} s^{-1} (solid line). The distribution corrected for the "Browne & Marchã (BM) effect" (i.e. the misclassification of optically faint BL Lacs whose light is swamped by the host galaxy) is also shown (dashed line). To reduce the statistical noise, these results represent the average of 10 simulation runs.

Fig. 14—The predicted V magnitude distribution for BL Lacs in a hypothetical ROSAT survey of about 300 deg^2 and $\nu_x \geq 2 \times 10^{-14}$ erg cm^{-2} s^{-1} (solid line). The distribution corrected for the "Browne & Marchã (BM) effect" (i.e. the misclassification of optically faint BL Lacs whose light is swamped by the host galaxy) is also shown (dashed line). To reduce the statistical noise, these results represent the average of 10 simulation runs.

Figure 1

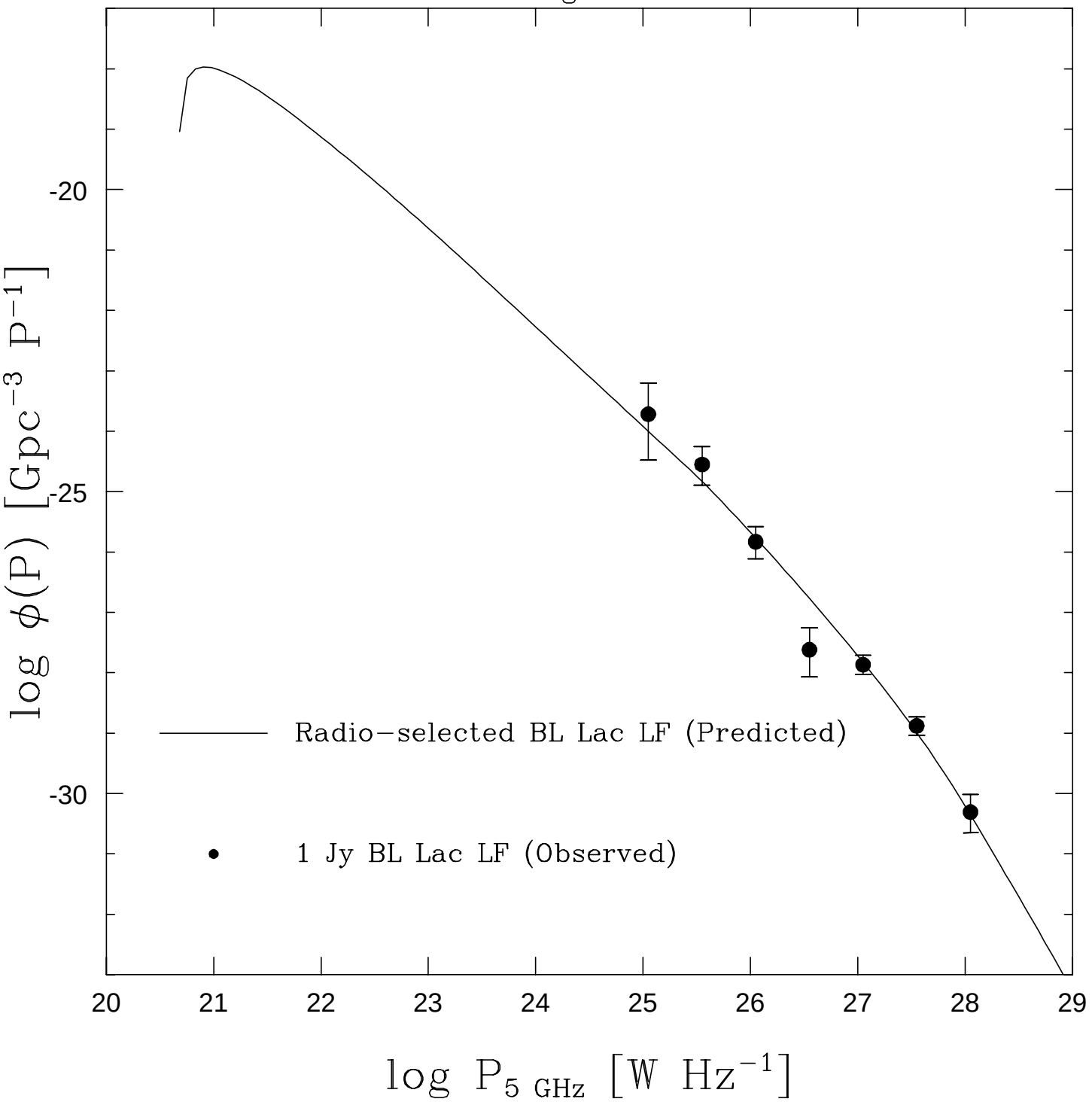
-20
-25
-30
log φ(P) [Gpc^{-3} P^{-1}]
Radio−selected BL Lac LF (Predicted)
1 Jy BL Lac LF (Observed)
20
21
22
23
24
25
26
27
28
29
log P$_{5\ GHz}$ [W Hz^{-1}]

Figure 2

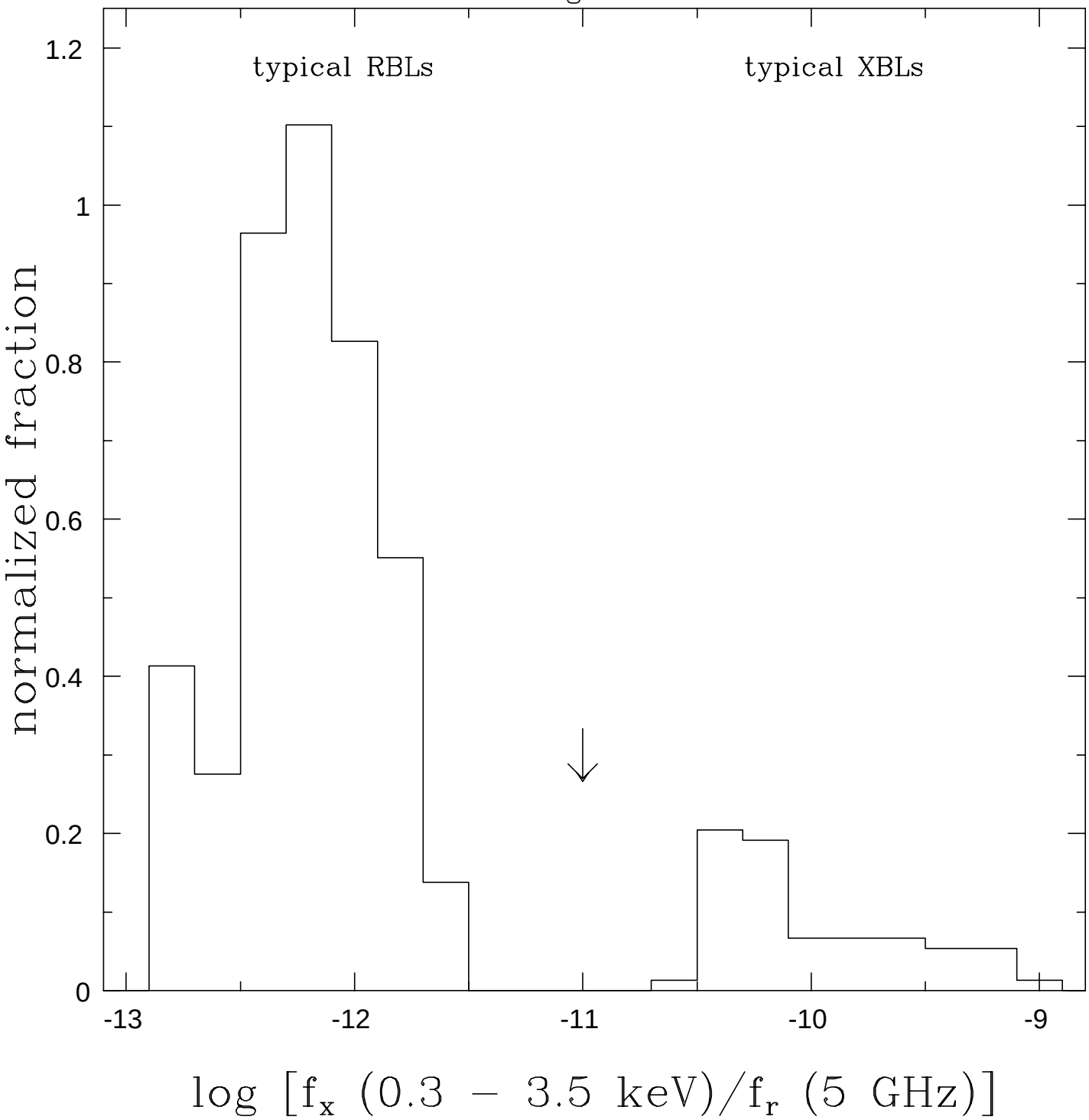
typical RBLs
typical XBLs
normalized fraction
1.2
1
0.8
0.6
0.4
0.2
0
-13
-12
-11
-10
-9
log [f_x (0.3 – 3.5 keV)/f_r (5 GHz)]

Figure 3

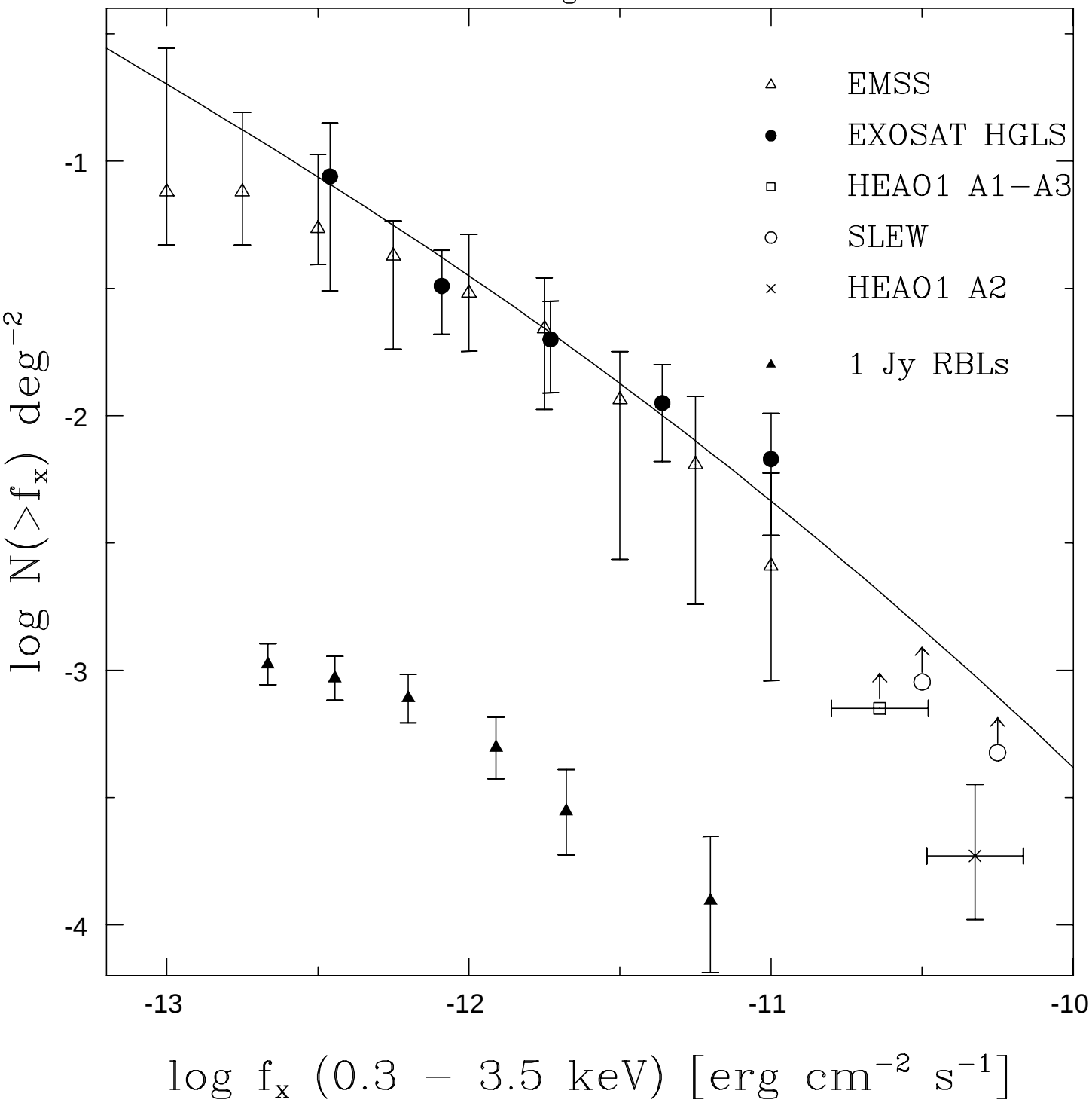
EMSS
EXOSAT HGLS
HEAO1 A1−A3
SLEW
HEAO1 A2
1 Jy RBLs
-1
-2
-3
-4
-13
-12
-11
-10
log N(>f_x) deg^-2
log f_x (0.3 − 3.5 keV) [erg cm^-2 s^-1]

Figure 4

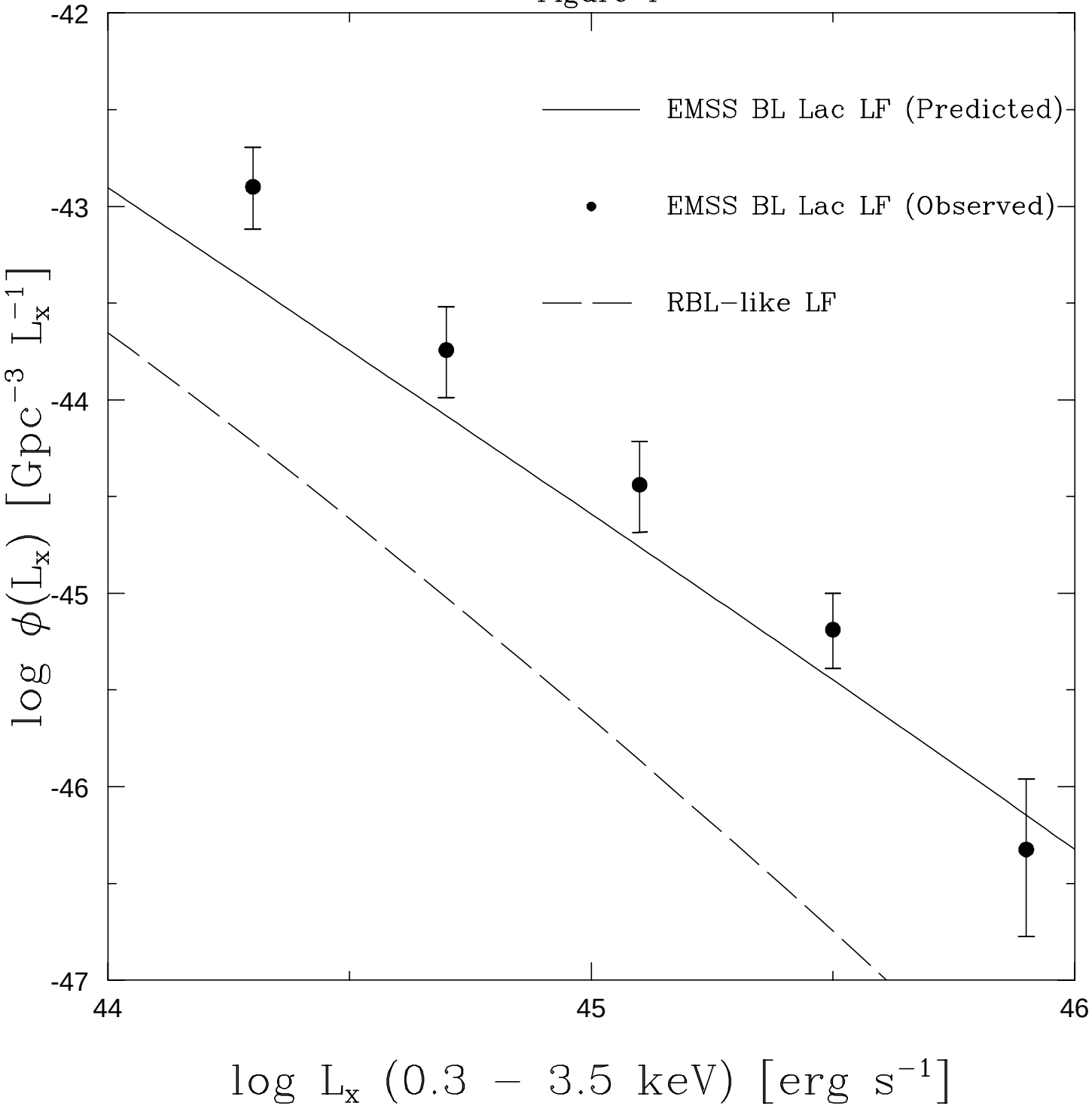
EMSS BL Lac LF (Predicted)
EMSS BL Lac LF (Observed)
RBL−like LF
-42
-43
-44
-45
-46
-47
44
45
46
log $\phi(L_x)$ [Gpc^{-3} L_x^{-1}]
log L_x (0.3 − 3.5 keV) [erg s^{-1}]

Figure 5

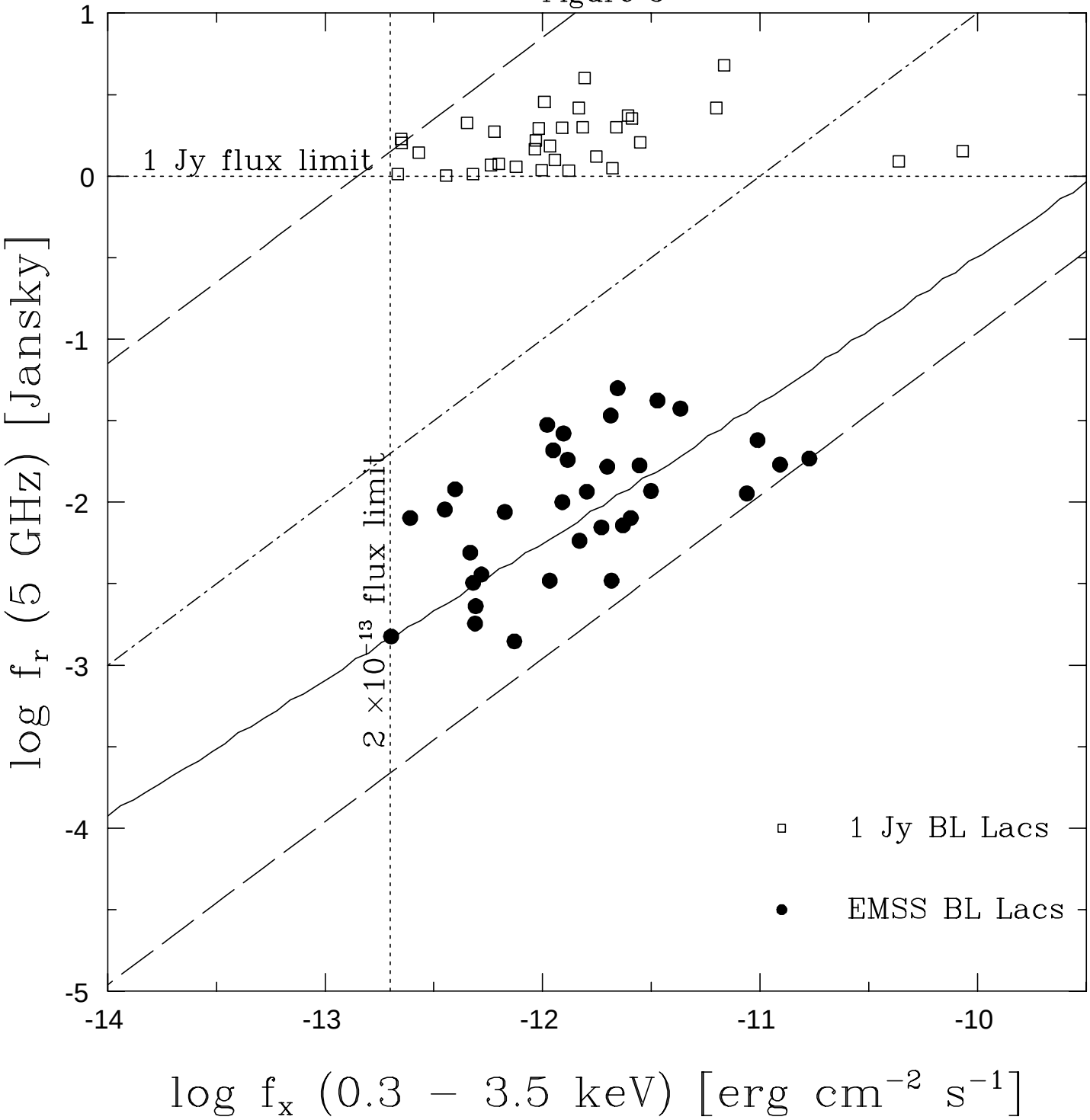
1 Jy flux limit
2 ×10⁻¹³ flux limit
1 Jy BL Lacs
EMSS BL Lacs
log f_r (5 GHz) [Jansky]
log f_x (0.3 − 3.5 keV) [erg cm⁻² s⁻¹]
1
0
-1
-2
-3
-4
-5
-14
-13
-12
-11
-10

Figure 6

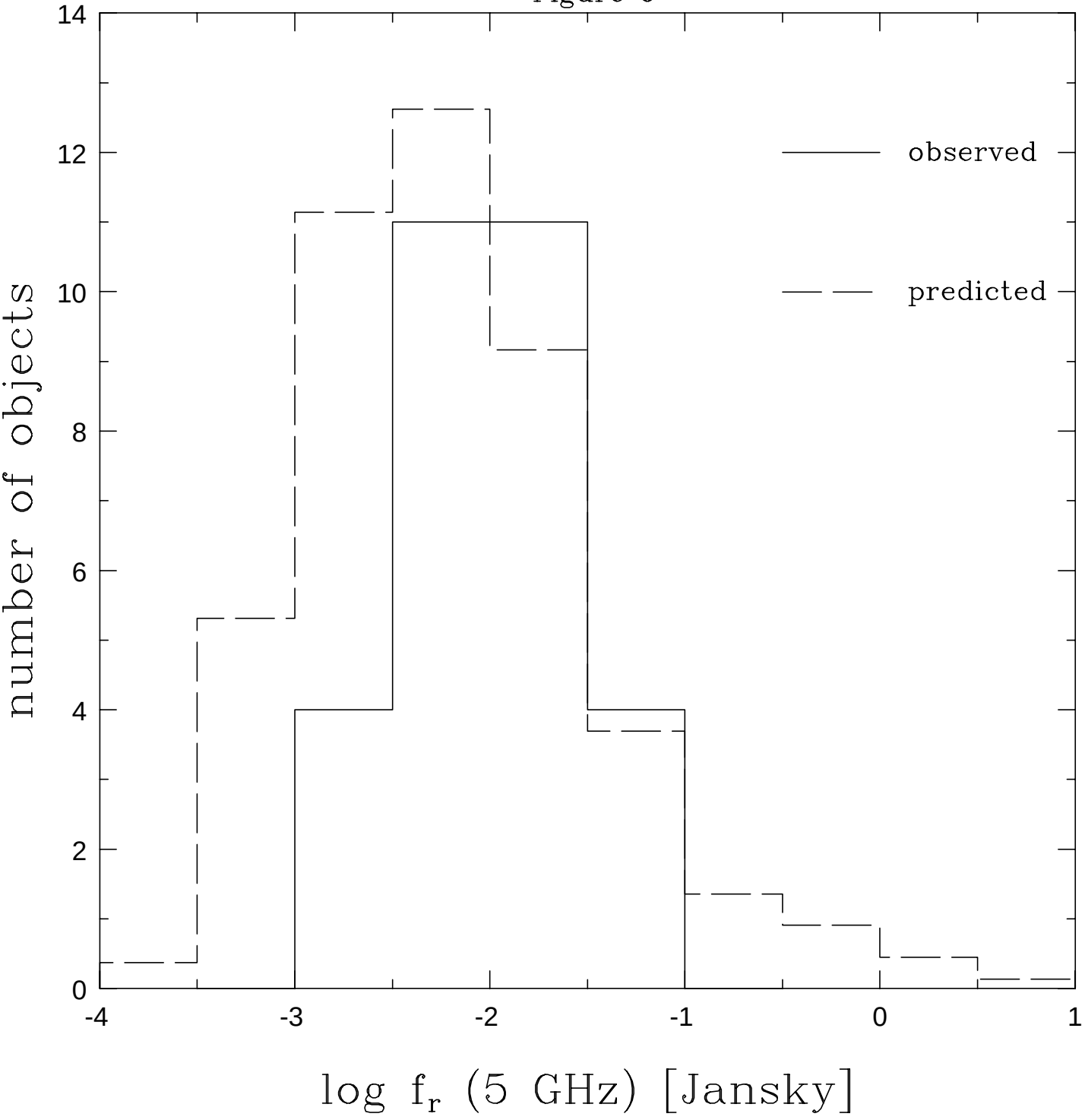
14
12
10
8
6
4
2
0
-4
-3
-2
-1
0
1
number of objects
log f_r (5 GHz) [Jansky]
observed
predicted

Figure 7

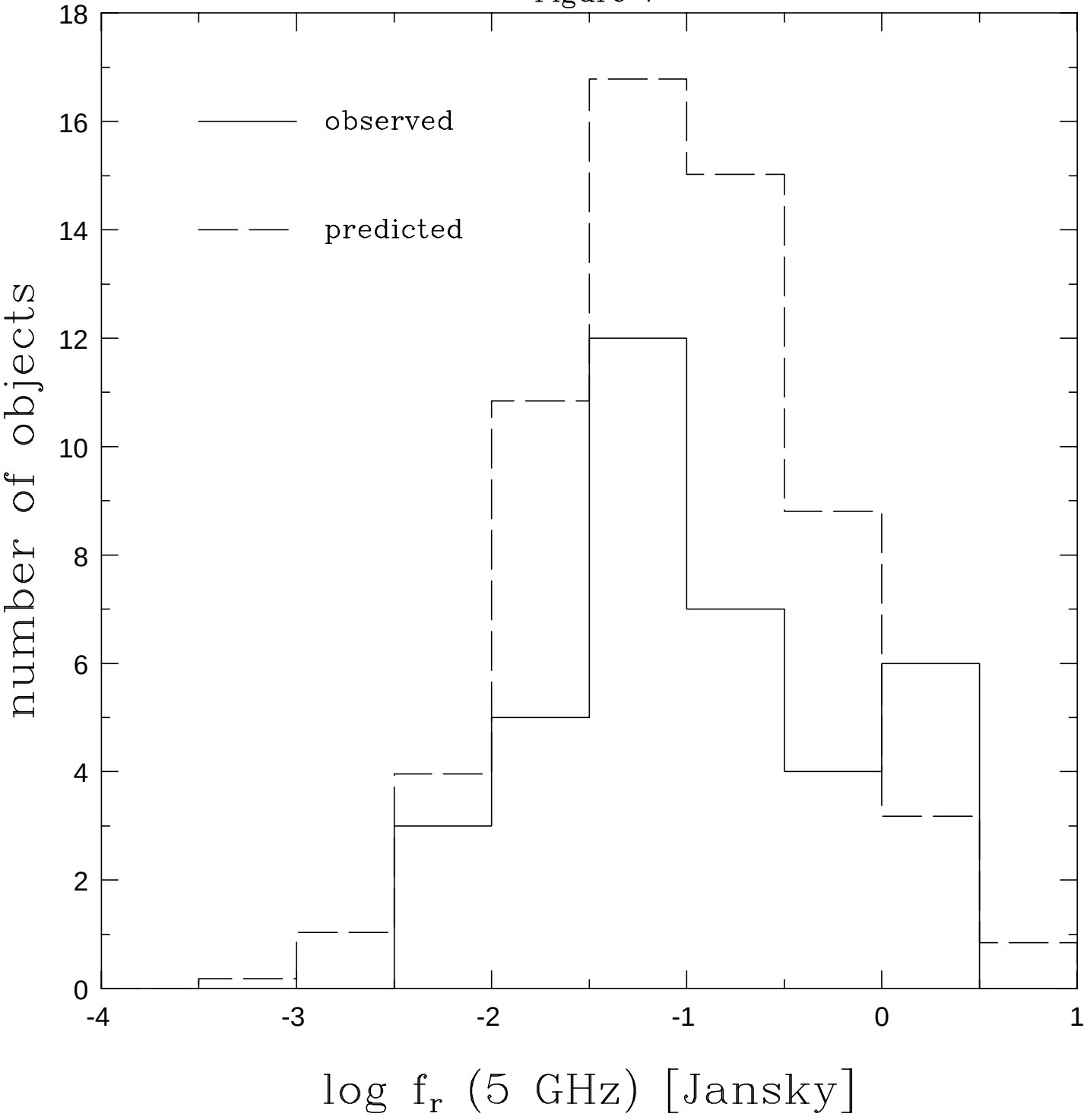
observed
predicted
number of objects
log f_r (5 GHz) [Jansky]
0
2
4
6
8
10
12
14
16
18
-4
-3
-2
-1
0
1

Figure 8

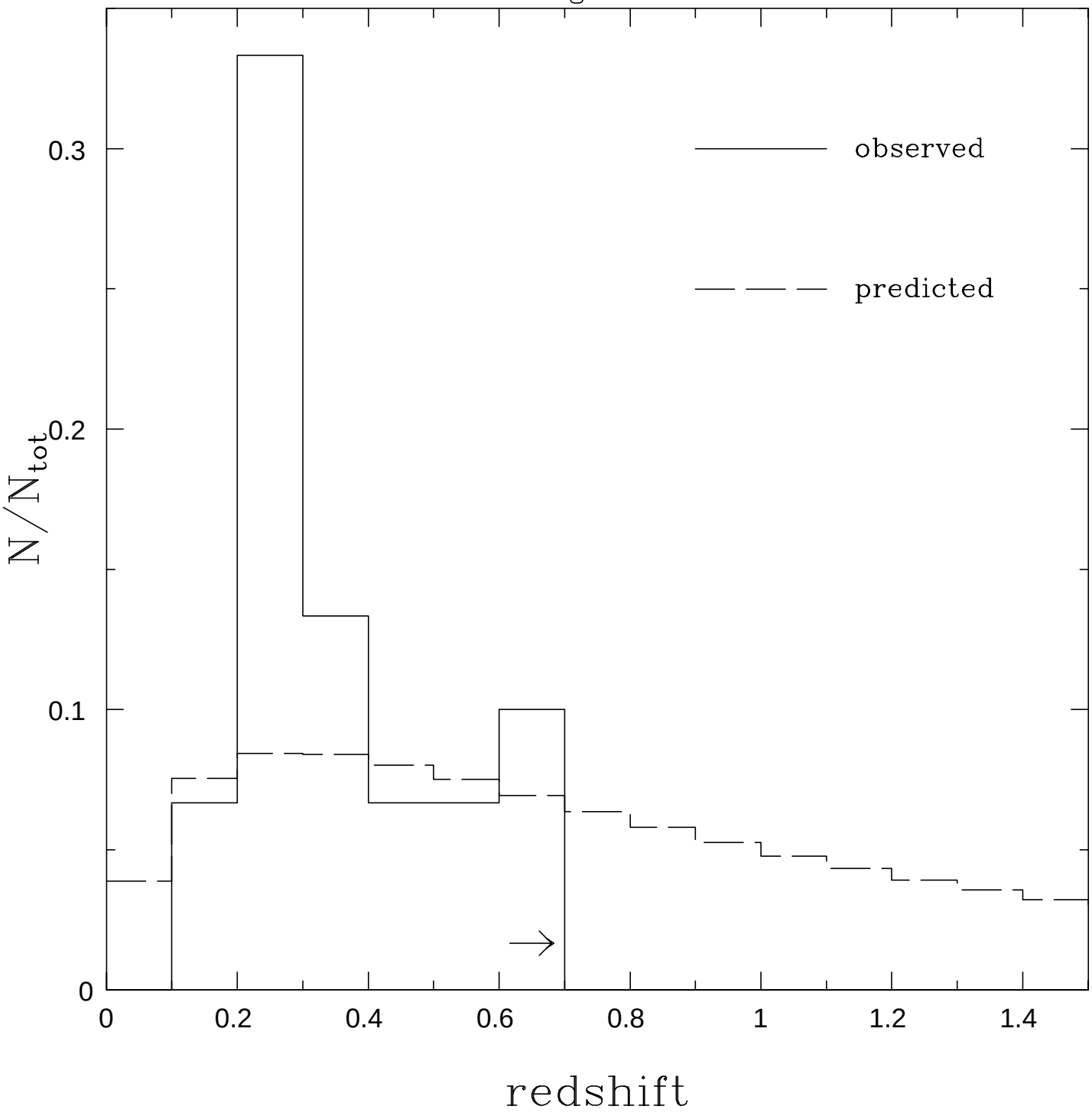
observed
predicted
0.3
0.2
0.1
0
N/N_{tot}
0
0.2
0.4
0.6
0.8
1
1.2
1.4
redshift

Figure 9

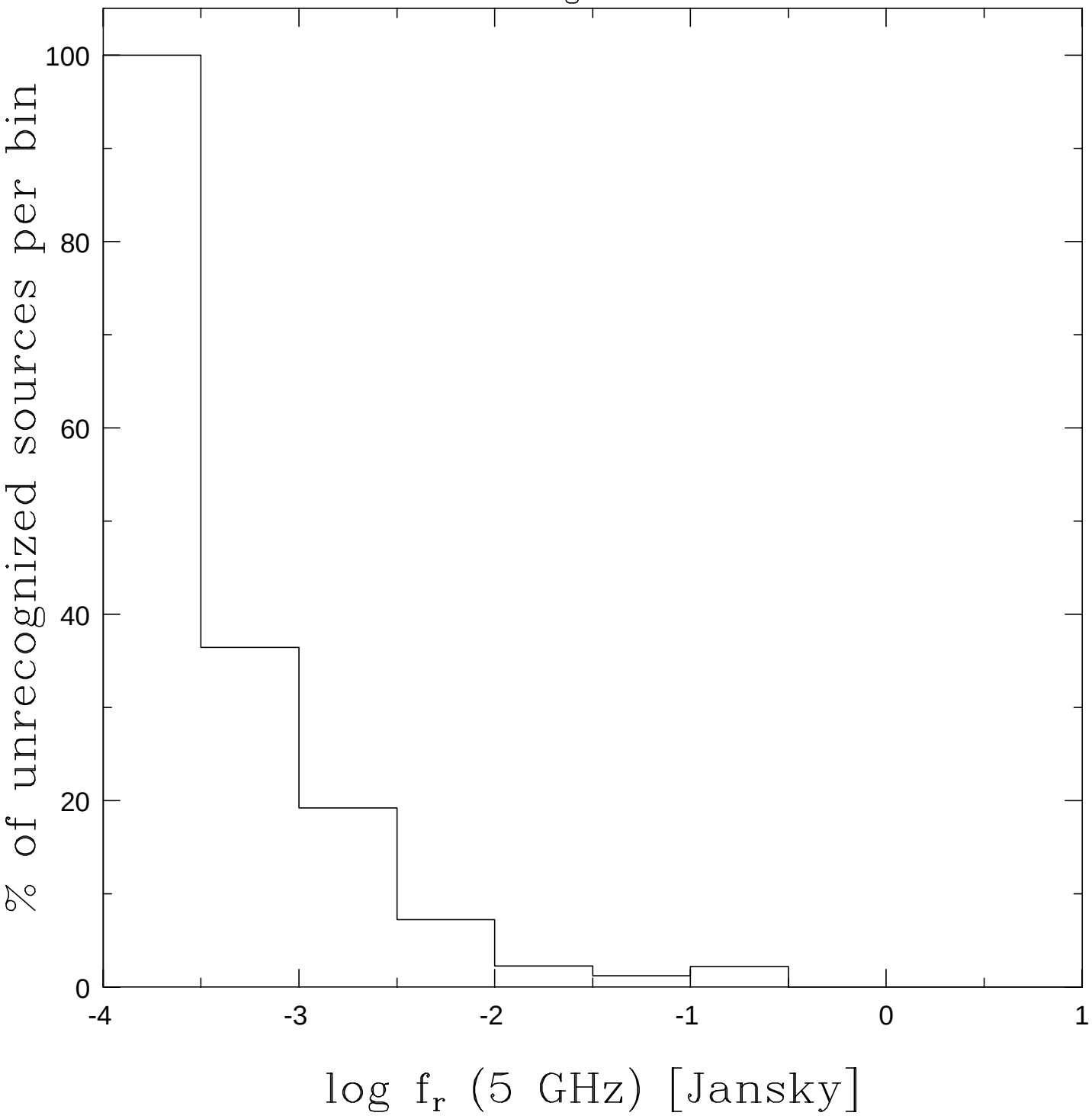
100
80
60
40
20
0
% of unrecognized sources per bin
-4
-3
-2
-1
0
1
log f_r (5 GHz) [Jansky]

Figure 10

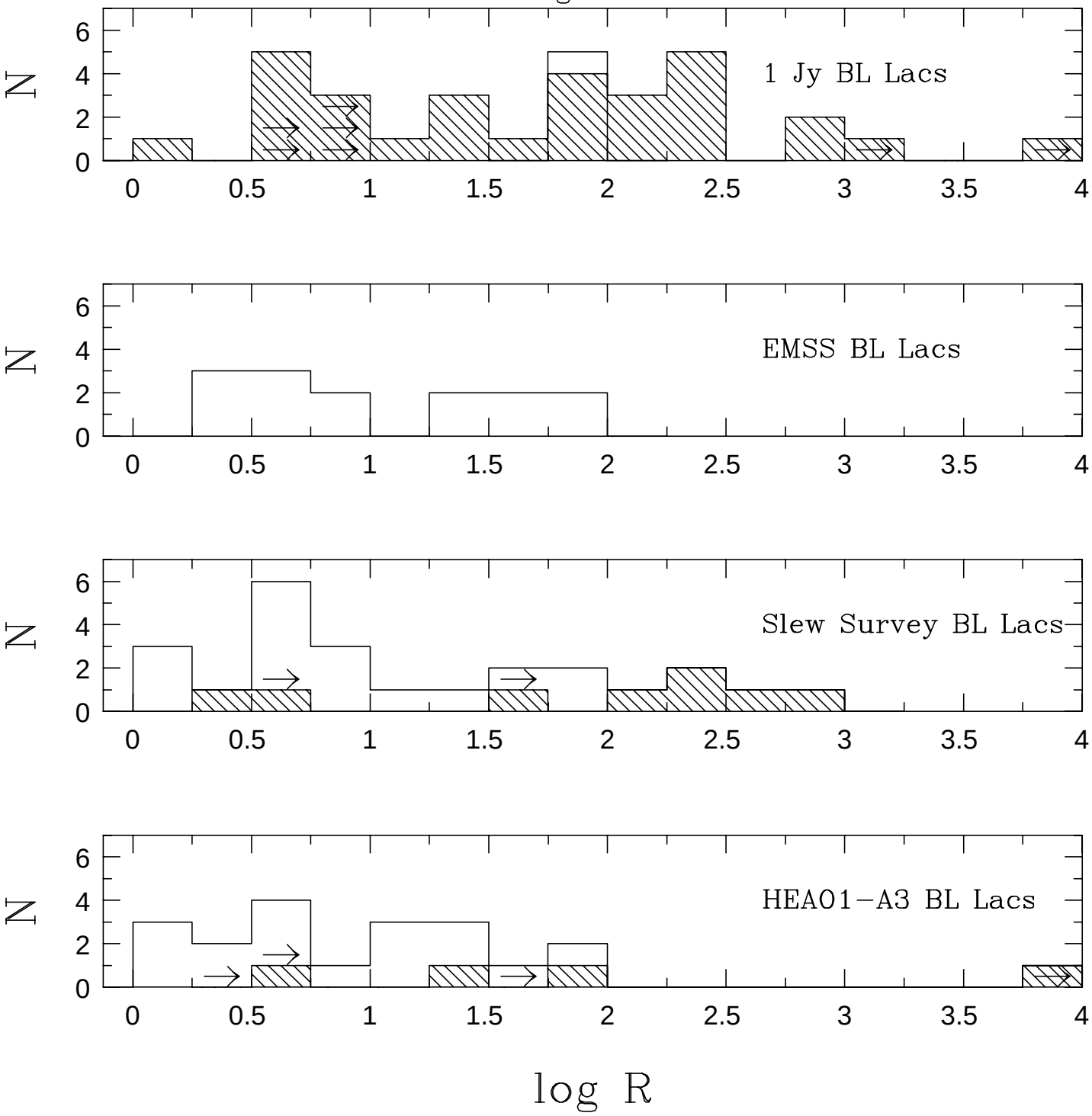
1 Jy BL Lacs
EMSS BL Lacs
Slew Survey BL Lacs
HEAO1−A3 BL Lacs
N
log R
0
2
4
6
0
0.5
1
1.5
2
2.5
3
3.5
4

Figure 11

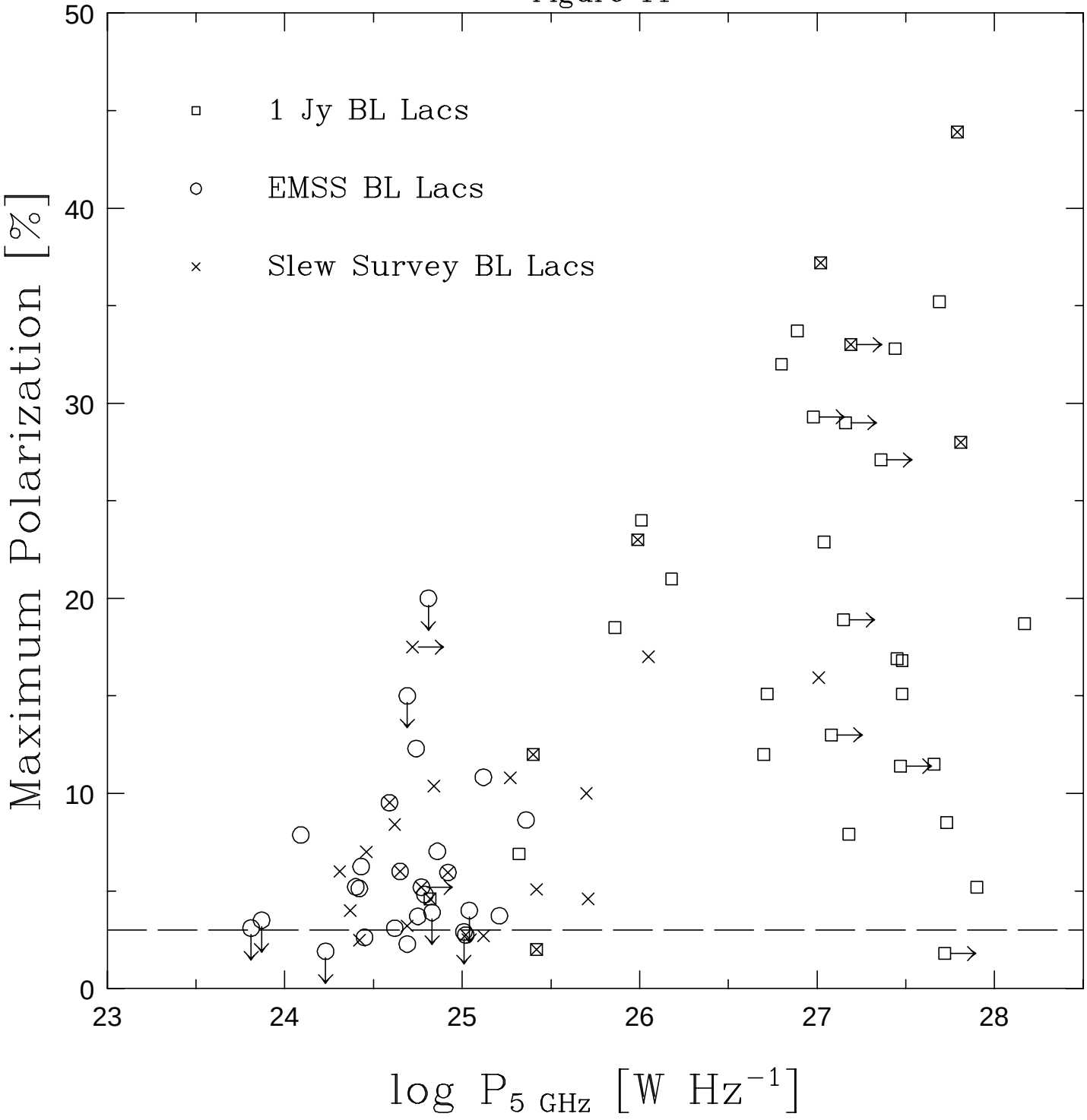
1 Jy BL Lacs
EMSS BL Lacs
Slew Survey BL Lacs
Maximum Polarization [%]
log P5 GHz [W Hz−1]
0
10
20
30
40
50
23
24
25
26
27
28

Figure 12

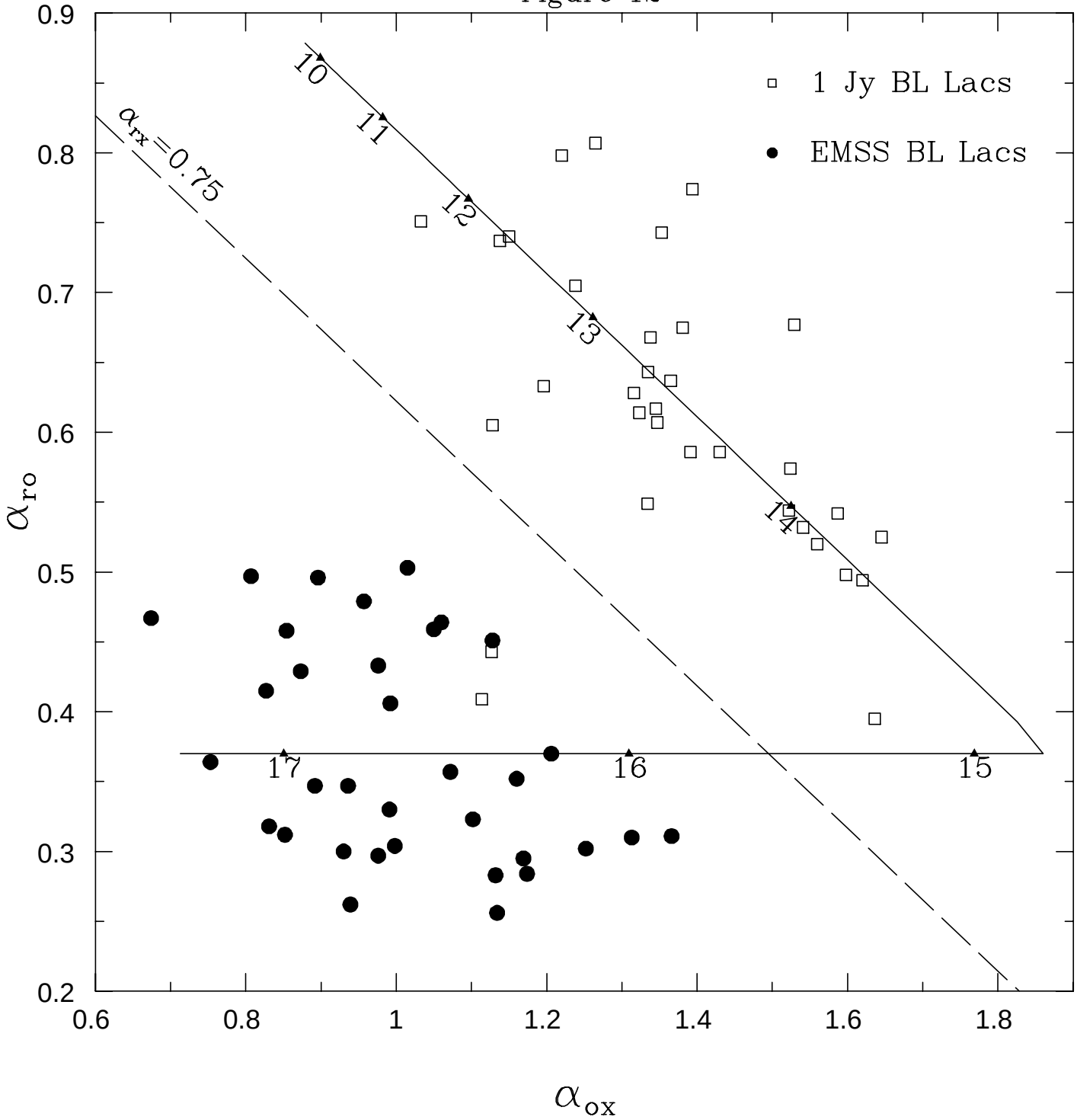
1 Jy BL Lacs
EMSS BL Lacs
$\alpha_{rx}=0.75$
10
11
12
13
14
15
16
17
α_{ro}
α_{ox}
0.9
0.8
0.7
0.6
0.5
0.4
0.3
0.2
0.6
0.8
1
1.2
1.4
1.6
1.8

Figure 13

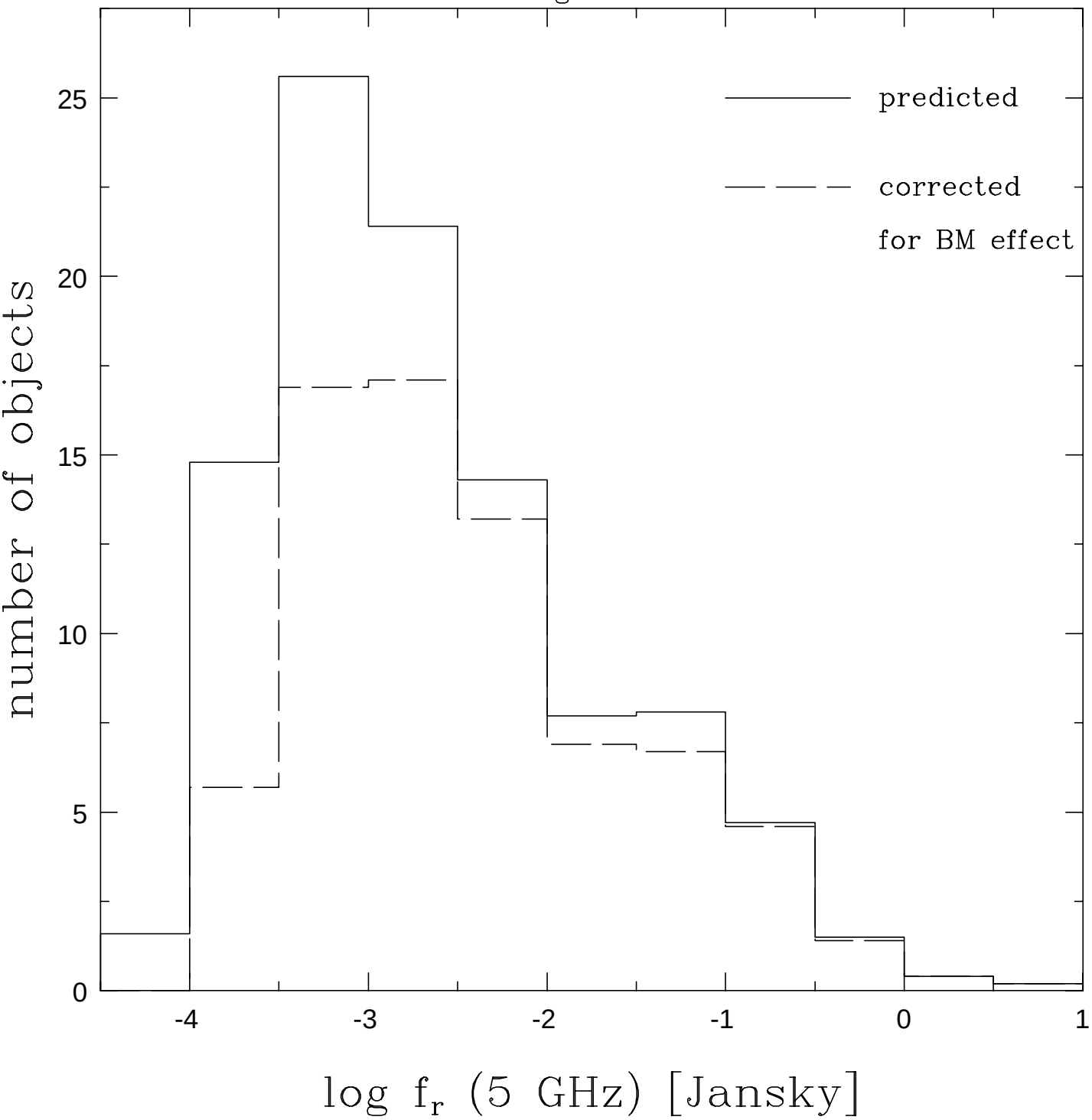
predicted
corrected
for BM effect
number of objects
0
5
10
15
20
25
-4
-3
-2
-1
0
1
log f_r (5 GHz) [Jansky]

Figure 14

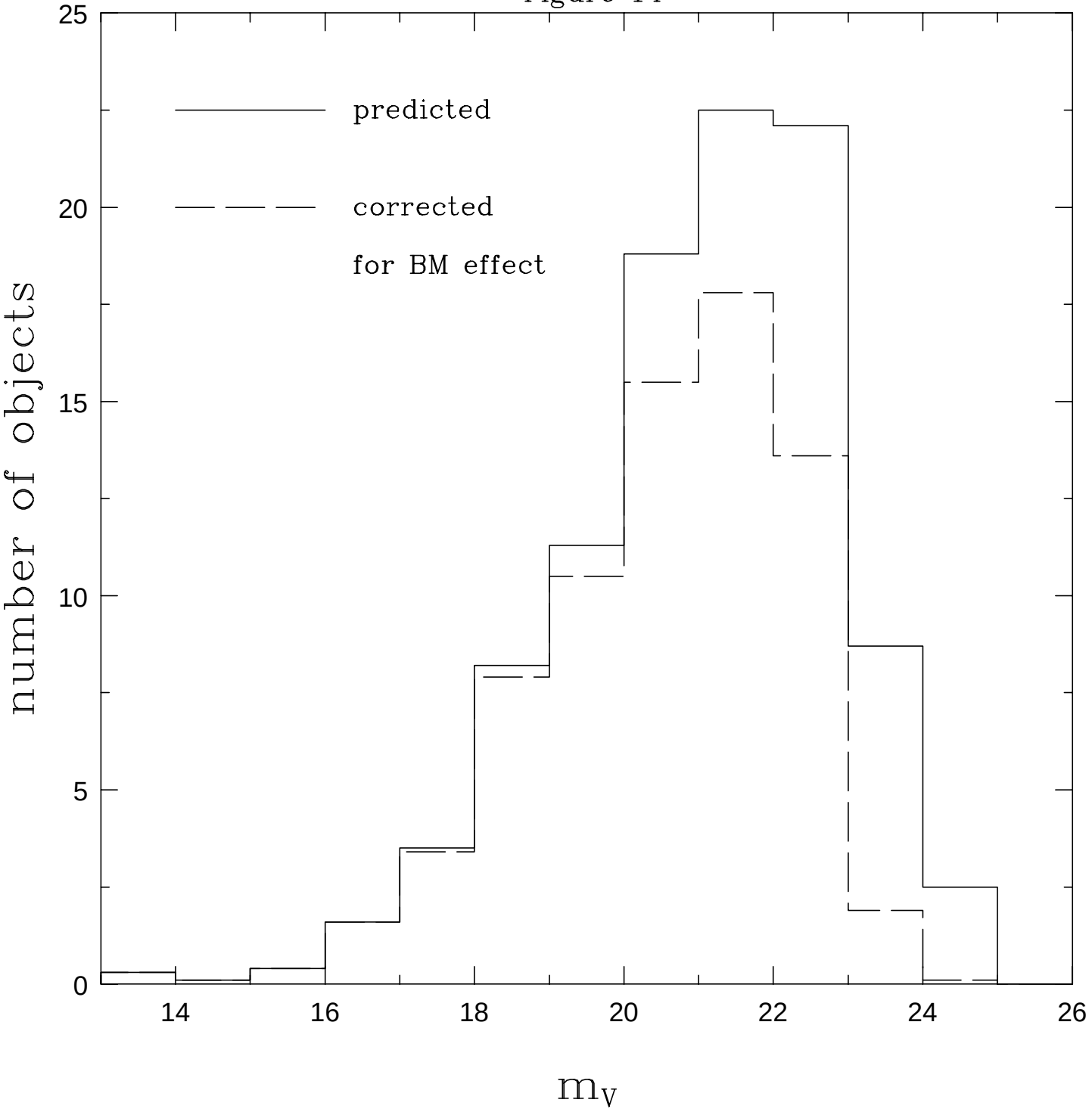
predicted
corrected
for BM effect
number of objects
m_V
0
5
10
15
20
25
14
16
18
20
22
24
26